

The Analysis of Space-Time Structure in QCD Vacuum II: Dynamics of Polarization and Absolute X -Distribution

Andrei Alexandru¹, Terrence Draper², Ivan Horváth² and Thomas Streuer³

¹The George Washington University, Washington, DC, USA

²University of Kentucky, Lexington, KY, USA

³University of Regensburg, Regensburg, Germany

Abstract

We propose a framework for quantitative evaluation of dynamical tendency for polarization in arbitrary random variable that can be decomposed into a pair of orthogonal subspaces. The method uses measures based on comparisons of given dynamics to its counterpart with statistically independent components. The formalism of previously considered X -distributions is used to express the aforementioned comparisons, in effect putting the former approach on solid footing. Our analysis leads to definition of a suitable correlation coefficient with clear statistical meaning. We apply the method to the dynamics induced by pure-gluon lattice QCD in local left-right components of overlap Dirac eigenmodes. It is found that, in finite physical volume, there exists a non-zero physical scale in the spectrum of eigenvalues such that eigenmodes at smaller (fixed) eigenvalues exhibit convex X -distribution (positive correlation), while at larger eigenvalues the distribution is concave (negative correlation). This *chiral polarization scale* thus separates a regime where dynamics enhances chirality relative to statistical independence from a regime where it suppresses it, and gives an objective definition to the notion of “low” and “high” Dirac eigenmode. We propose to investigate whether the polarization scale remains non-zero in the infinite volume limit, in which case it would represent a new kind of low energy scale in QCD.

1 Introduction

In physics it is sometimes useful to decompose a multi-component variable/quantity with respect to a pair of orthogonal subspaces spanning its range. Examples relevant for the area of application that we target here, namely QCD and its vacuum structure, include the decomposition of a bispinor into left-right chirality components, and the decomposition of the gauge field strength tensor into self-dual and anti-self-dual parts. Physical reasons for considering such decompositions usually have to do with the fact that the dynamics of the variable involves (or is expected to involve) a specific type of relation among such suitably defined projections. The expected correlations can then be tested in a relevant physical experiment or evaluated in theoretical calculations.

The property of polarization, namely the tendency for asymmetric participation of the two subspaces in the preferred values of the variable, is frequently of interest in the above context. While the qualitative meaning of the concept is obvious, the ways to characterize and quantify the degree of polarization in the dynamics are highly non-unique *a priori*. One typically operates under the implicit assumption that the physical context uniquely “selects the tools”, i.e. that the choice of the polarization characteristics is driven by the physical nature of the quantity at hand. There are situations however, the study of QCD vacuum structure being one of them, where we may be interested in polarization characteristics that pertain to dynamics alone and are not conditioned on which specific physical situation the dynamics is modelling. Our goal in this paper is to develop a framework to describe and quantify such *dynamical tendency for polarization*. In addition to being free of kinematic effects, we also require that the framework provides a possibility for high level of detail. In other words, we are not only interested in a suitable average polarization parameter, but rather want the aspects of polarization to be separated from other content of the dynamics.

To construct our formalism, we will build upon the X -distribution proposal of Ref. [1] which grew from similar motivations albeit with a specific aim to characterize the local chirality of QCD Dirac eigenmodes. The X -distribution approach is based on the following logic. Consider the left-right decomposition $\psi = \psi_L + \psi_R$ of the local value in the eigenmode, and some function $\mathcal{X} \equiv \mathcal{X}(\psi_L, \psi_R)$ that reflects the degree of chiral polarization in ψ . Since \mathcal{X} is defined at every space-time point, it is a local characteristic providing the information on changes in the left-right polarization within the mode. The equilibrium ensemble of QCD gauge configurations induces the distribution of associated \mathcal{X} -values for chosen sets of eigenmodes.¹ In other words, denoting by X an independent variable whose domain is in the range of \mathcal{X} , there exists a function $P(X)$, namely the probability distribution of the polarization characteristic specified by \mathcal{X} . The X -distribution $P(X)$ provides rather detailed information about the chiral polarization properties of the selected group of modes.

While the concept of X -distributions is suitable for our purposes, the issue of “dynamical versus kinematical” has not been explicitly addressed in that framework. The channel through which kinematics enters here is the function \mathcal{X} since there is a large freedom in choosing measures that qualitatively reflect chiral polarization. Rather than analyzing this freedom, the related work was carried out with the implicit rationale that the proper fixed choice of this *polarization function* can be made. For example, the original definition in Ref. [1] involved \mathcal{X} linear in the polar angle of point $(|\psi_L|, |\psi_R|)$ from the “left-right plane” (chiral orientation parameter). This was used in most of the early follow-up works [2] with some departures [3, 4]. However, especially in the case of Dirac eigenmodes, it is not entirely clear which physical consideration should fix the selection. Thus, focusing exclusively on the dynamics, in the sense discussed above, provides a meaningful direction to proceed in.

With the above discussion in mind, we wish to propose a construct that (1) provides a detailed differential information on polarization modeled after the X -distribution but (2) doesn't rely on a fixed polarization function \mathcal{X} , and (3) reflects only the dynamics. Note that while the involvement of kinematics proceeds via the polarization function \mathcal{X} , requirement (2) only represents a necessary condition for this characteristic to be considered purely

¹In the early works, additional constraints to define sub-ensembles of \mathcal{X} -values, such as restrictions to space-time regions with strong fields, were frequently used.

dynamical. Indeed, we view the concept of “dynamical” in this context as entailing a specific meaning of “correlational” or, in more general terms, based on some form of comparison to statistical independence. This is why the requirements (2) and (3) are listed separately and need to be fulfilled simultaneously.

To satisfy these requirements, we first reinterpret the X -distribution as a relative measure. In other words, we show that one can view $P(X)$ not only as an object assigned to given dynamics and the polarization function, but also as an object comparing this dynamics to another dynamics associated with the polarization function in question. We develop a formalism that allows us to switch freely between the two interpretations which, in technical terms, allows us to construct an X -distribution for arbitrary pair of dynamics. Equipped with this tool, we then proceed to define a truly dynamical characteristic as a relative X -distribution assigned to dynamics of interest and the related one where left and right components are chosen independently of one another from corresponding marginal distributions. Note that the latter is the needed point of comparison representing statistical independence. The crucial point, implicitly embedded in this procedure, is that it is independent of the polarization function used to carry it out. In other words, while the implementation must proceed via some polarization function \mathcal{X} , the final result doesn’t depend on this choice. We thus refer to the above dynamical characteristic as an *absolute X -distribution* in order to distinguish it from the original one that can only be viewed in a relative sense.²

In terms of requirement (3), one can draw a parallel between our construction and the definition of the Pearson correlation coefficient for random variables q_1, q_2 governed by a joint probability distribution $\mathcal{P}(q_1, q_2)$, namely $r \equiv (\langle q_1 q_2 \rangle - \langle q_1 \rangle \langle q_2 \rangle) / (\sigma_1 \sigma_2)$, with σ_1, σ_2 being the corresponding standard deviations. Computing just $\langle q_1 q_2 \rangle$ will not convey any dynamical information (it won’t tell us anything about tendencies of the relationship between q_1 and q_2), nor does this value have any specific statistical meaning. However, after the subtraction of “uncorrelated relationship” $\langle q_1 \rangle \langle q_2 \rangle$, the resulting covariance acquires a qualitative dynamical content. Finally, the normalization via standard deviations, ensuring that $-1 \leq r \leq 1$, gives the coefficient a well-defined statistical meaning, and thus a quantitative dynamical significance. In effect, the dynamical construct that we propose implements the “subtraction of statistical independence” at the level of distributions which, among other things, has an added bonus that proper normalizations are automatically in place.

With absolute X -distribution at hand, one can naturally define an averaged quantity based on it, and this role is played by the *correlation coefficient of polarization* (CCP). CCP has a clear statistical meaning in that it is linearly related to the probability that the sample chosen from the distribution governing the dynamics is more polarized than the sample chosen from its counterpart with statistically independent components. One utility of CCP is that it naturally ranks (orders) possible dynamics with respect to the polarization. In particular, larger CCP means larger dynamical tendency for polarization. Moreover, the positive CCP signals that the dynamics enhances the polarization relative to statistical independence, while the negative value means that polarization is being dynamically suppressed. Due to its absolute nature, we propose CCP as a basic “figure of merit” quantifying polarization properties inherent to dynamics.

²One can also refer to this construct as the *dynamical X -distribution*, explicitly emphasizing the fact that its purpose is to remove any kinematical content from the description of polarization.

As a first application of the above techniques, we analyze local chiral properties of low-lying QCD Dirac eigenmodes. It was already the motivation of Ref. [1] that local properties of these modes are expected to be connected to low-energy features of QCD, especially to those related to spontaneous chiral symmetry breaking. However, our goals in this investigation are quite different from those of Ref. [1]. Rather than checking the consistency of assumptions for certain models, as we did in Ref. [5] which contains the preliminary discussion of techniques developed here, our aim is to build a model-independent information on relevant properties of these modes in line with the *bottom-up* approach to QCD vacuum structure as formulated in Ref. [6]. Indeed, it is the purpose of this series [7] to contribute to developing the set of techniques that can facilitate these goals.

The summary of our main initial findings on the chiral polarization properties of low-lying overlap Dirac eigenmodes are as follows. The absolute X -distributions of the lowest modes are convex on their domain, while the X -distributions of higher modes are concave. This implies that the lowest modes exhibit a dynamical tendency for chirality (positive CCP) while the higher modes dynamically suppress it (negative CCP). At fixed volume and lattice spacing, there exists a transition point $\Lambda_T(V, a)$ in the spectrum where the absolute X -distribution is strictly flat, and the polarization properties are indistinguishable from statistical independence. Based on four lattice spacings, our data supports the proposition that this scale remains finite in the continuum limit, i.e. $\lim_{a \rightarrow 0} \Lambda_T(V, a) = \Lambda_T(V) > 0$ for $V < \infty$. The appearance of this sharply-defined new feature in the QCD Dirac spectrum could be relevant for understanding the mechanism of spontaneous chiral symmetry breaking.

The structure of the paper is as follows. We start by discussing an explicit example of the absolute X -distribution calculation in Sec. 2. Our goal here is to provide a concise introduction to the method with sufficient practical and conceptual information for it to be directly applied to the problem of interest here, namely the study of local chiral properties in overlap Dirac eigenmodes. This application and corresponding results are then described in Sec. 3. In Appendix A we describe in detail the theoretical structure, the meaning and the scope of absolute polarization methods proposed here. This is a rather extensive topic of its own, and the section can be read independently of the QCD content. Indeed, this discussion is carried out in a completely generic setting, emphasizing the universal applicability of the formalism to any area where the concept of polarization plays relevant role.

2 Absolute X -Distribution – a Primer

Given that our first application of absolute polarization methods targets chiral properties of Dirac eigenmodes, we will use the specifics of that setting to introduce the approach. For definiteness, consider the set of lattice Dirac eigenmodes comprised of lowest two (non-zero) conjugate pairs on gauge backgrounds from ensemble E_1 of Table 1.³ Collecting all local values ψ from these modes into single pool, let us consider the associated collection of two-component objects (q_1, q_2) , namely the magnitudes of left and right components of ψ

$$(q_1, q_2) \equiv (|\psi_L|, |\psi_R|) \quad \psi_L \equiv \frac{1}{2}(1 - \gamma_5) \psi \quad \psi_R \equiv \frac{1}{2}(1 + \gamma_5) \psi \quad (1)$$

³Details concerning the parameters of lattice gauge ensembles and lattice Dirac operator are given in Sec. 3 and are not important for this discussion.

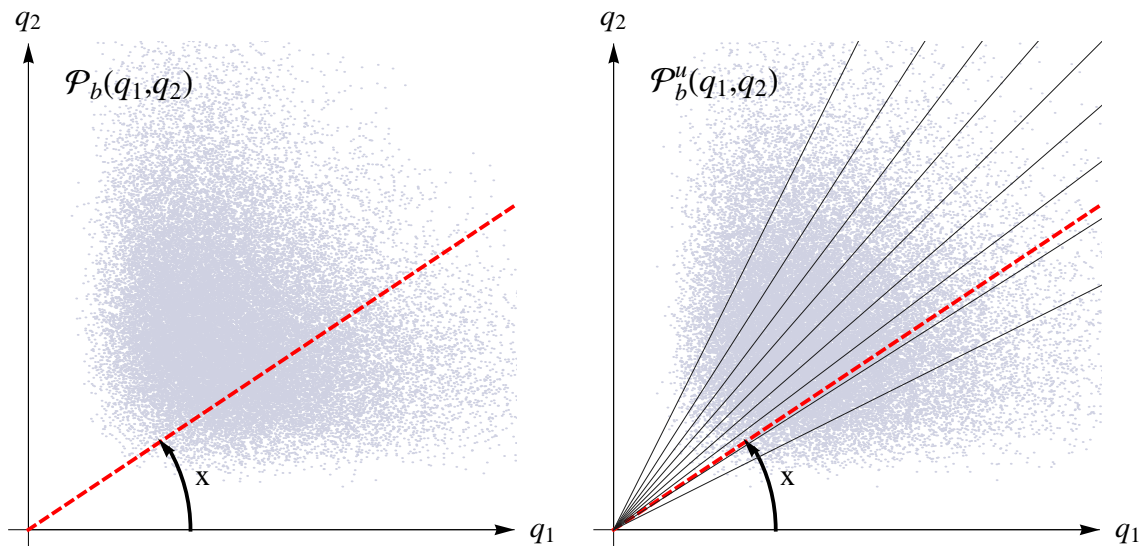


Figure 1: Left: Dynamics governing the polarization properties of two lowest modes for ensemble E_1 . Right: The associated “uncorrelated” dynamics; solid gray lines separate the quadrant into 10 sectors, each containing 10% of the population.

The distribution of these “samples” is shown on the left side of Fig. 1, and statistically approximates the underlying *base* probability distribution $\mathcal{P}_b(q_1, q_2)$ describing the limit of infinite gauge statistics.

One can assess a degree of polarization in a given sample by its polar angle $\varphi \in [0, \pi/2]$ which is convenient to symmetrize into *reference polarization coordinate*, namely [1]

$$x \equiv \frac{4}{\pi} \varphi - 1 \quad x \in [-1, 1] \quad (2)$$

Note that strictly left-polarized and strictly right-polarized samples are characterized by values $x = -1$ and $x = +1$ respectively. The probability distribution $P_r(x)$ of polarization coordinate over the population of samples is sometimes invoked as a detailed measure characterizing chiral polarization properties of Dirac modes in question, and is usually referred to as the (reference) X -distribution [1]. Our goal is to define a construct of similar nature which however focuses on the relation of the dynamics in question to the “uncorrelated” one where left and right components of $\psi = (\psi_L, \psi_R)$ are paired with one another at random from available pool of possibilities. Indeed, such comparative polarization measure could then be viewed as *dynamical*. Note that the needed point of comparison (the population of statistically independent components) associated with our exemplary dynamics is shown on the right side of Fig. 1. It approximates the underlying distribution $\mathcal{P}_b^u(q_1, q_2) \equiv p(q_1)p(q_2)$ with $p(q)$ being the distribution of a single component in original $\mathcal{P}_b(q_1, q_2)$. This uncorrelated dynamics carries its own reference X -distribution $P_r^u(x)$.

To obtain the polarization measure of the above kind, we perform a differential comparison of polarization in $\mathcal{P}_b(q_1, q_2)$ relative to $\mathcal{P}_b^u(q_1, q_2)$ as follows. A ray passing through the origin can be specified by its reference polarization coordinate x , as shown in Fig. 1. Determine the fraction of population contained between the q_1 -axis and this ray, separately for

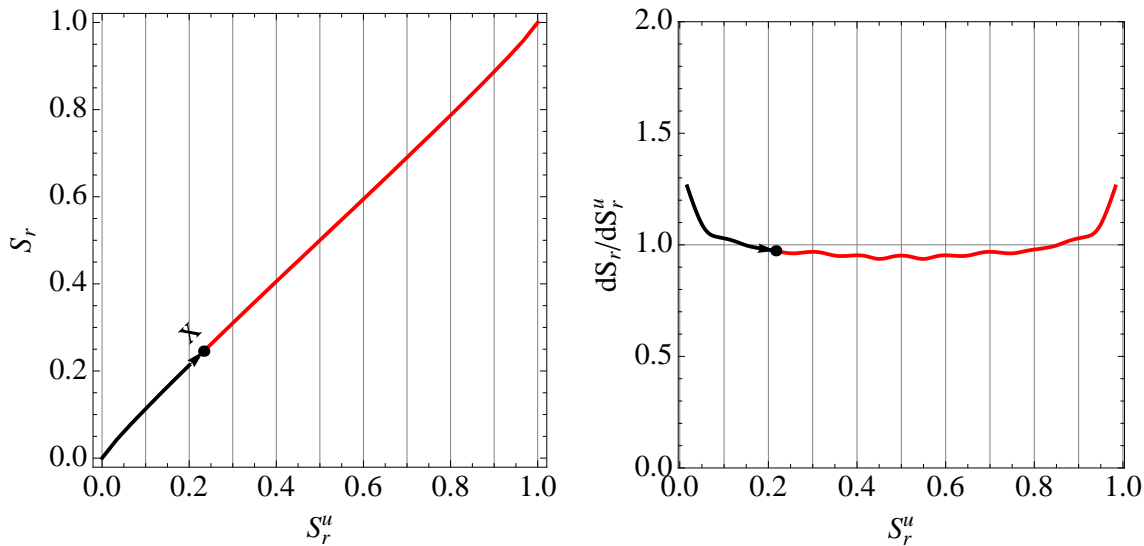


Figure 2: Steps in the construction of absolute X -distribution for data shown in Fig. 1. See the discussion in the text.

\mathcal{P}_b and \mathcal{P}_b^u . These fractions represent the cumulative probability functions $S_r(x)$ and $S_r^u(x)$ associated with $P_r(x)$ and $P_r^u(x)$ respectively. Eliminating x , every line is represented by a point in the cumulative distribution plane (S_r^u, S_r) with the set of all such points forming a graph starting at $(0,0)$ and ending at $(1,1)$. If the two situations (“dynamics”) in question had identical polarizations, the graph would be a straight line. On the left side of Fig. 2 we plot the result of this construction for data displayed in Fig. 1. One can see that the correlated and uncorrelated dynamics have very similar polarizations since the graph is close to being linear. To obtain a differential comparison, and to better see the differences, we compute the slope of the cumulative polarization graph and show it on the right side of Fig. 2. Since this dependence represents a probability distribution in variable S_r^u , we can see that the correlated case exhibits a small excess of probability with respect to the uncorrelated one (the horizontal line) near the extremal values. Noting that the extremal values $S_r^u = 0, 1$ actually correspond to strictly polarized cases $x = -1, 1$ respectively, the observed qualitative behavior of the slope graph in fact conveys the excess of polarization in dynamics described by $\mathcal{P}_b(q_1, q_2)$ relative to dynamics described by $\mathcal{P}_b^u(q_1, q_2)$. To standardize this polarization characteristic, we finally convert the distribution in S_r^u into distribution in rescaled polarization-like variable $S_r^u \rightarrow 2S_r^u - 1 \equiv X$ whose domain is $[-1, 1]$. The resulting construct $P_A(X)$ will be referred to as the *absolute X -distribution*.

We now wish to make several remarks regarding the above method.

(i) Performing a practical calculation of absolute X -distribution with uniform resolution in X requires that we evaluate cumulative probabilities at values x_i that split the uncorrelated population into N_b bins of equal size. This is indicated on the right hand side of Fig. 1 for $N_b = 10$ by the rays enclosing 10% of population each, and similarly by vertical lines in Fig. 2. The corresponding reference distribution $P_r(X \equiv x)$ and absolute X -distribution $P_A(X)$ computed with this resolution are shown in Fig. 3.

(ii) As one can readily inspect, the above geometric construction would lead to the same re-

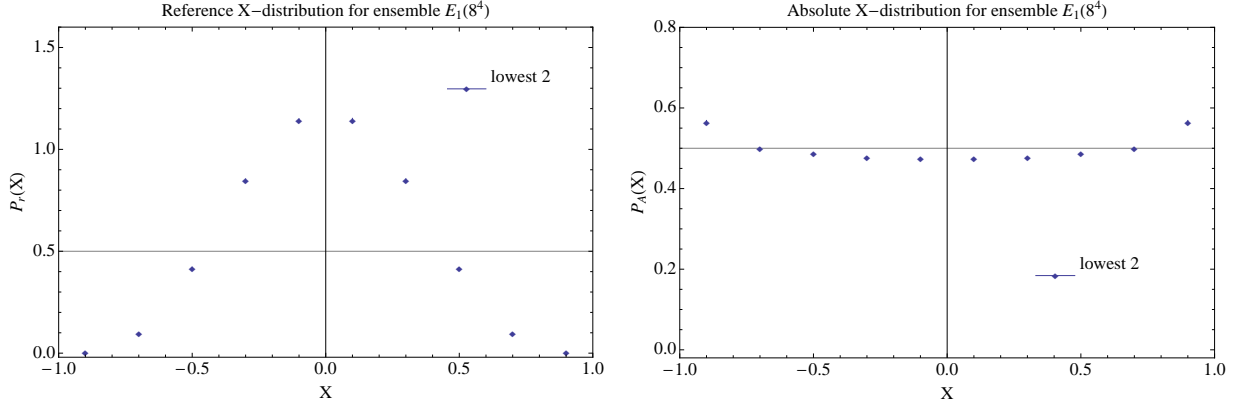


Figure 3: Reference X -distribution (left) and absolute X -distribution (right) for data shown in Fig. 1 with resolution of 10 bins.

sult had we decided to quantify the degree of chiral polarization in ψ by some arbitrary *polarization function* $\mathcal{X}(x)$ rather than by the default choice $\mathcal{X}(x) = x$. Indeed, such different possibilities correspond to different parametric representations of the same curve in the (S_r^u, S_r) plane, and this information drops out of the calculation. The associated *reparametrization invariance* is significant since it expresses the fact that the proposed description of polarization is independent of the “language” (or “reference frame”) chosen to represent the concept at the sample level. This is necessary for the description to be considered purely dynamical and reflects the absolute nature of this construction.

(iii) The definition of absolute X -distribution given above is equivalent to constructing the X -distribution of Ref. [1], but associated with polarization function

$$\mathcal{X}_A(x) \equiv 2 \int_{-1}^x dy P_r^u(y) - 1 \quad (3)$$

This makes the fact that the absolute X -distribution represents a valid polarization measure more explicit. In fact, depending on the dynamics $\mathcal{P}_b(q_1, q_2)$ in question, the procedure adjusts the polarization characteristic so that it directly measures deviations relative to uncorrelated dynamics. In this language, the reparametrization invariance of absolute X -distribution follows from the fact that \mathcal{X}_A is invariant under the choice of reference polarization coordinate as one can directly verify.

(iv) We wish to emphasize that the strong dependence on the choice of the polarization function (dependence on “kinematics”) provided a major motivation for extending the old X -distribution approach in the direction described here. Indeed, as discussed extensively in Appendix A, even qualitative conclusions can be entirely misleading if one relies only on the X -distribution associated with fixed polarization function. This is illustrated in Fig. 11 where a suitable choice of polarization function can either produce seemingly clear chiral double-peaking or what appears as completely non-chiral single peak.

(v) In addition to detailed description of polarization contained in absolute X -distribution, we also define a single figure of merit reflecting the overall dynamical tendency for polariza-

tion, namely

$$C_A \equiv 2 \int_{-1}^1 dX |X| P_A(X) - 1 \quad (4)$$

The positive value of this *correlation coefficient of polarization* $C_A \in [-1, 1]$ indicates that the dynamics enhances polarization relative to randomness, while the negative value implies its dynamical suppression. Indeed, as one can check (see Appendix A), C_A is linearly related to the probability that the sample chosen from $\mathcal{P}_b(q_1, q_2)$ is more polarized than the sample (independently) chosen from $\mathcal{P}_b^u(q_1, q_2)$, leading to the above interpretation.

The elements described in this section are at the core of the general dynamical polarization method we are proposing in this work. Formal definitions and detailed discussion of the logical structure involved are given in Appendix A. While the concise overview given in this section is sufficient to apply the method to the case of QCD Dirac eigenmodes in what follows, we emphasize that the content of Appendix A is important not only for deeper understanding the scope and the meaning of the approach, but also for its practical application in case of singular polarization dynamics.

3 QCD Dirac Eigenmodes

We will now apply the absolute polarization methods to the case of low-lying QCD Dirac eigenmodes in a more systematic manner. As argued extensively e.g. in Ref. [1], the properties of these modes are expected to encode many important features of QCD vacuum. Their direct connection to spontaneous chiral symmetry breaking, beyond the Banks–Casher relation [8], is particularly anticipated.

We perform our exploratory calculations in the context of pure glue lattice QCD with Iwasaki gauge action [9]. The left side of Table 1 summarizes the parameters of our five ensembles. Lattice scale has been determined from the string tension following the methods and results of Ref. [10]. Ensembles E_1 – E_4 have fixed physical volume, and are intended for investigation of the continuum limit. Ensemble E_5 has larger physical volume and serves mainly to check whether our qualitative conclusions remain stable in that regard.

Ensemble	Size	N_{config}	Volume	Lattice Spacing	$\Lambda_{\text{LOW}}^{\text{MAX}}$	$\Lambda_{\text{LOW}}^{\text{AVE}}$	$\Lambda_{\text{HIGH}}^{\text{MIN}}$	$\Lambda_{\text{HIGH}}^{\text{AVE}}$
E_1	8^4	100	$(1.32 \text{ fm})^4$	0.165 fm	449	226	1956	1980
E_2	12^4	97	$(1.32 \text{ fm})^4$	0.110 fm	407	169	1711	1735
E_3	16^4	99	$(1.32 \text{ fm})^4$	0.0825 fm	304	142	1513	1553
E_4	24^4	96	$(1.32 \text{ fm})^4$	0.055 fm	344	136	1338	1366
E_5	16^4	99	$(1.76 \text{ fm})^4$	0.110 fm	162	58	1087	1123

Table 1: The summary of five ensembles used in overlap eigenmode calculations. The right side of the table describes some properties of the spectra (in MeV) with $\Lambda_{\text{LOW}}^{\text{AVE}}$ denoting the average magnitude of lowest near-zero eigenvalue over the ensemble and $\Lambda_{\text{HIGH}}^{\text{AVE}}$ denoting the same for highest eigenvalue. $\Lambda_{\text{LOW}}^{\text{MAX}}$ is the magnitude of the maximal lowest eigenvalue, and $\Lambda_{\text{HIGH}}^{\text{MIN}}$ the magnitude of the minimal highest eigenvalue.

Low-lying eigenmodes of the overlap Dirac operator [11] were calculated on gauge backgrounds from the above ensembles. Specifically, we used the massless overlap operator with Wilson kernel, the negative mass parameter $\rho = 26/19$ ($\kappa = 0.19$), and Wilson parameter $r = 1$. The eigenmodes and eigenvalues were computed using our own implementation of the implicitly restarted Arnoldi algorithm with deflation [12]. The zero modes and about 50 pairs of lowest near-zero modes⁴ with complex-conjugated eigenvalues were obtained for each configuration. The right side of Table 1 compiles the information on spectral boundaries of computed regions for each ensemble (see the caption). Note that since zero modes are exactly chiral, it is the near-zero modes that are of interest here. They are in fact the relevant eigenmodes to consider in the context of spontaneous chiral symmetry breaking.

3.1 Reference and Absolute X -Distributions

In order to get the basic idea about the dynamical tendency for chirality in the obtained eigenmodes, we first focus on the lowest non-zero and highest computed modes. For this purpose, we collect into the “lowest” eigenmode group the two lowest near-zero modes for each configuration from the given gauge ensemble. Since the eigenmodes of conjugate pairs have identical chiral properties, we actually include one representative from each of the two lowest conjugate pairs. Similarly, the “highest” eigenmode group contains eigenmodes from the highest two pairs. The collection of all local values of (q_1, q_2) (magnitudes of left and right components) in the grouped eigenmodes represent the dynamics $\mathcal{P}_b(q_1, q_2)$ that we are investigating.

On the left side of Fig. 4 we show the reference X -distributions, or reference polarization dynamics, for “lowest” and “highest” eigenmodes in ensembles E_1 – E_4 . On the right side of the same figure are the associated X -distributions for the dynamics with statistically independent left-right components. A detailed description of the method used to obtain this “randomized” or “uncorrelated” dynamics is given in Appendix B, as are the other technical details related to the construction of absolute X -distributions.

Looking at the left side of Fig. 4, the most obvious feature is the narrowing of the distributions going from low to higher modes. This is as expected from many studies of standard X -distributions even though we should point out that, contrary to most of such studies, here we are not making any restrictions based on magnitudes of $\psi(x)$. Rather, all local values are part of the dynamics, as they should be.

An interesting aspect of Fig. 4 is the comparison of left and right columns, i.e. the comparison of pure kinematics (right side) to kinematics combined with dynamics (left side). As one can see, the two are barely distinguishable implying that the qualitative appearance of reference X -distributions is almost entirely driven by kinematics. In order to expose the dynamical polarization tendencies, we construct the corresponding absolute X -distributions that effectively remove the features due to kinematics. The resulting distributions are shown in Fig. 5 with lowest modes on the left and highest modes on the right.

One can easily interpret the absolute X -distributions since the uncorrelated dynamics is represented by the uniform distribution shown as a solid horizontal line. Thus, for the

⁴The exact number of computed near-zero mode pairs depends on the number of zero modes (topological charge) of a given configuration. If N_0 is the number of zero modes then there were $55 - N_0$ pairs computed.

lowest modes, there is an enhancement of samples with largest polarization relative to statistical independence, and the corresponding suppression of samples with low polarization. In fact, one can read from the graph complete differential information on how much enhancement/suppression there is for arbitrary segment of uncorrelated population. The correlation coefficient of polarization (CCP) is obviously positive for the lowest modes, and the dynamics governing them exhibits the dynamical tendency for polarization. As can be inspected from the right column, this situation reverses for the highest computed modes in all lattice gauge ensembles. Indeed, in that case the dynamics suppresses samples with largest polarization and CCP is negative.

3.2 Convexity of Absolute X -Distributions

A characteristic feature of absolute X -distributions shown in Fig. 5, as well as of all the other ones that we computed from our ensembles, is that they are in some sense the simplest they can be. For example, while there doesn't seem to be a reason *a priori* excluding multiple intersections of $P_A(X)$ with uniform distribution on each “chiral half” (interval $[-1, 0]$ and $[0, 1]$), we have generically seen just one. Note that these crossings define segments in the sample space with dynamically enhanced/suppressed chirality. Moreover, consistently with the above, the absolute X -distributions for QCD eigenmodes seem to be either purely convex or purely concave on their domain $[-1, 1]$. This implies that they are also strictly monotonic on each chiral half.

To give a well-defined meaning to these kinds of observations, one should specify more precisely the dynamics of chiral pairs in question. In other words, one should specify how are the associated populations defined in terms of selected Dirac eigenvectors so that the corresponding characteristics are both physically meaningful and have proper continuum limits. In that regard, things simplify for lattice QCD in the infinite volume since one can assign an X -distribution to an individual eigenmode in that case, at least for equilibrium gauge backgrounds. Moreover, under standard assumptions, the local properties of such modes will not depend on the specific equilibrium configuration in question. Thus, in the infinite volume, the eigenvalue λ is the only label distinguishing the local behavior of Dirac eigenmodes in the underlying gauge theory. It is a common practice that the above is also mimicked in the finite volume, except that the gauge ensemble average has to be performed in that case. In other words, one defines properties of eigenmodes at scale Λ by inserting $\delta(\Lambda - |\lambda|)$ into the expression for ensemble average of an observable involving a spectral sum over individual eigenmodes ψ_λ .

Here we will follow the above logic and all the conclusions regarding the polarization properties of Dirac eigenmodes will implicitly refer to dynamics of modes at fixed Λ in the above sense.⁵ With that in mind we suggest the following for further investigation.

Proposition 1 (Convexity): The absolute X -distributions of low-lying overlap Dirac modes in $SU(3)$ pure glue lattice gauge theory are strictly convex, strictly concave or constant.

⁵Note that the practical implementation of this, i.e. the selection of appropriate eigenmodes with only finite gauge ensembles at our disposal, can vary depending on how much data is actually available. For example, our selection of “lowest” modes in the previous section could be viewed as a procedure to determine the behavior of eigenmodes at $\Lambda = 0$ in the continuum limit.

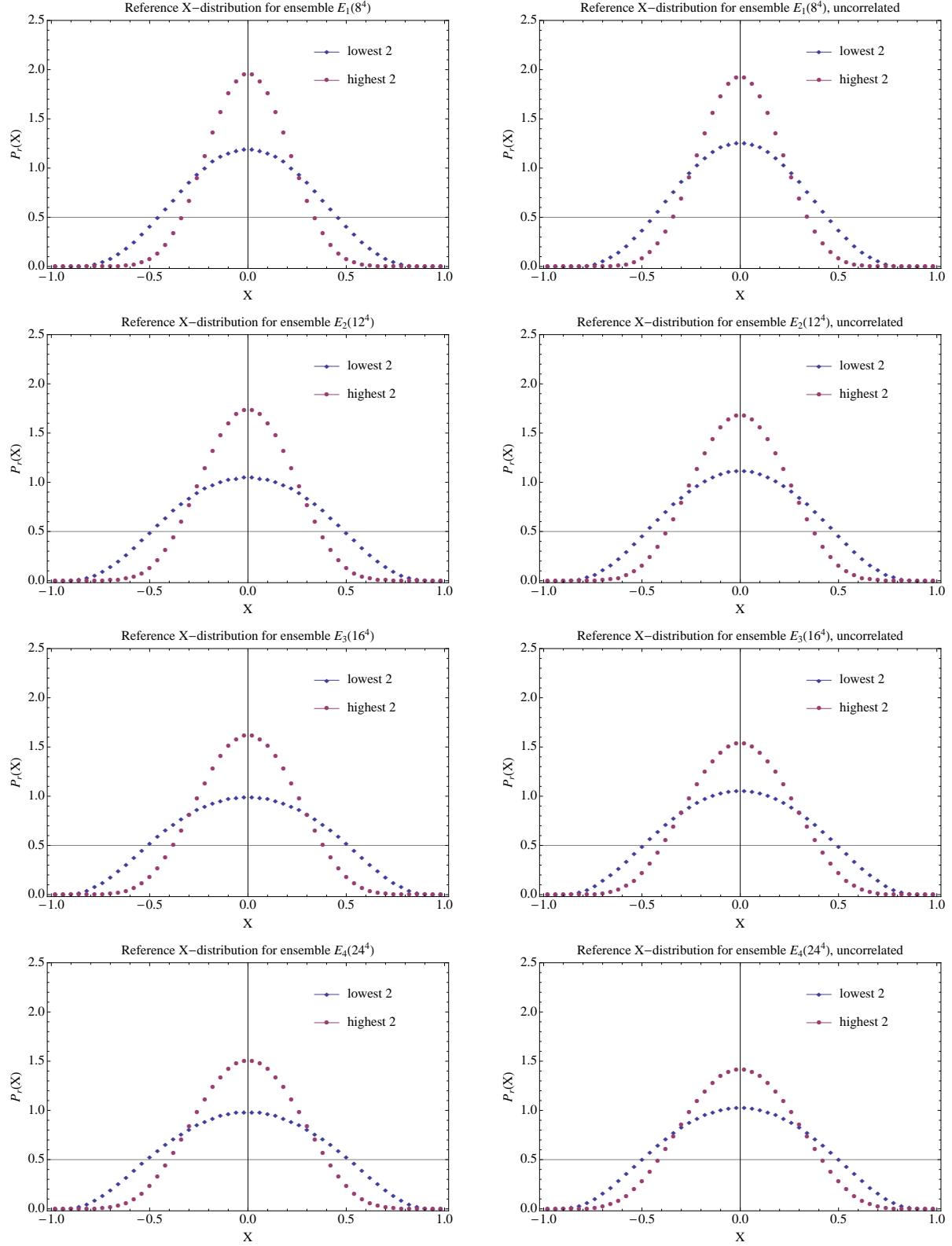


Figure 4: Reference X -distributions for “lowest” and “highest” modes in ensembles E_1 – E_4 are shown in the left column. The associated distributions with statistically independent left–right components (“uncorrelated”) are shown in the right column.

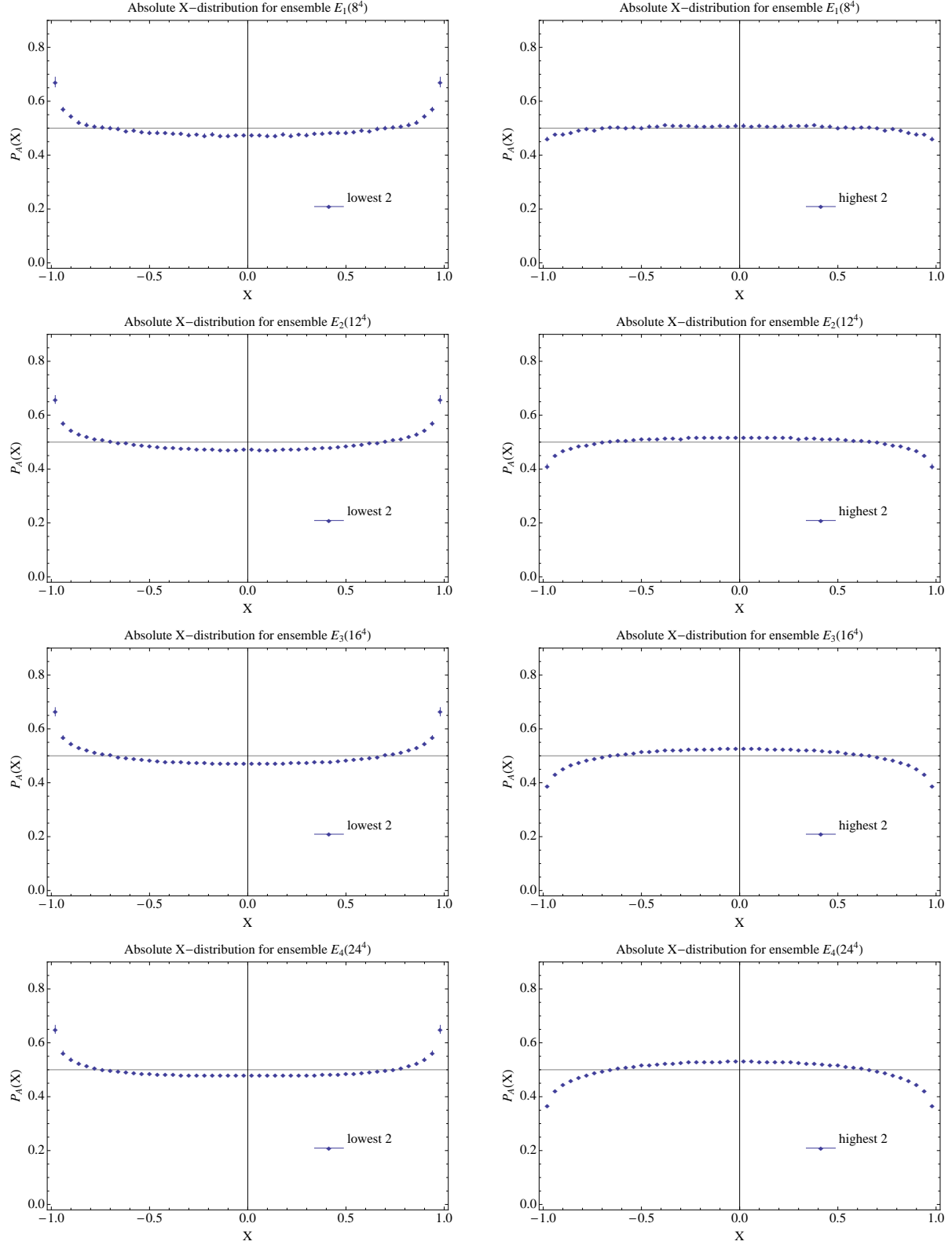


Figure 5: Absolute X -distributions for lowest (left column) and highest (right column) two pairs of modes for ensembles E_1 – E_4 . Lattice spacing is decreasing from top to down.

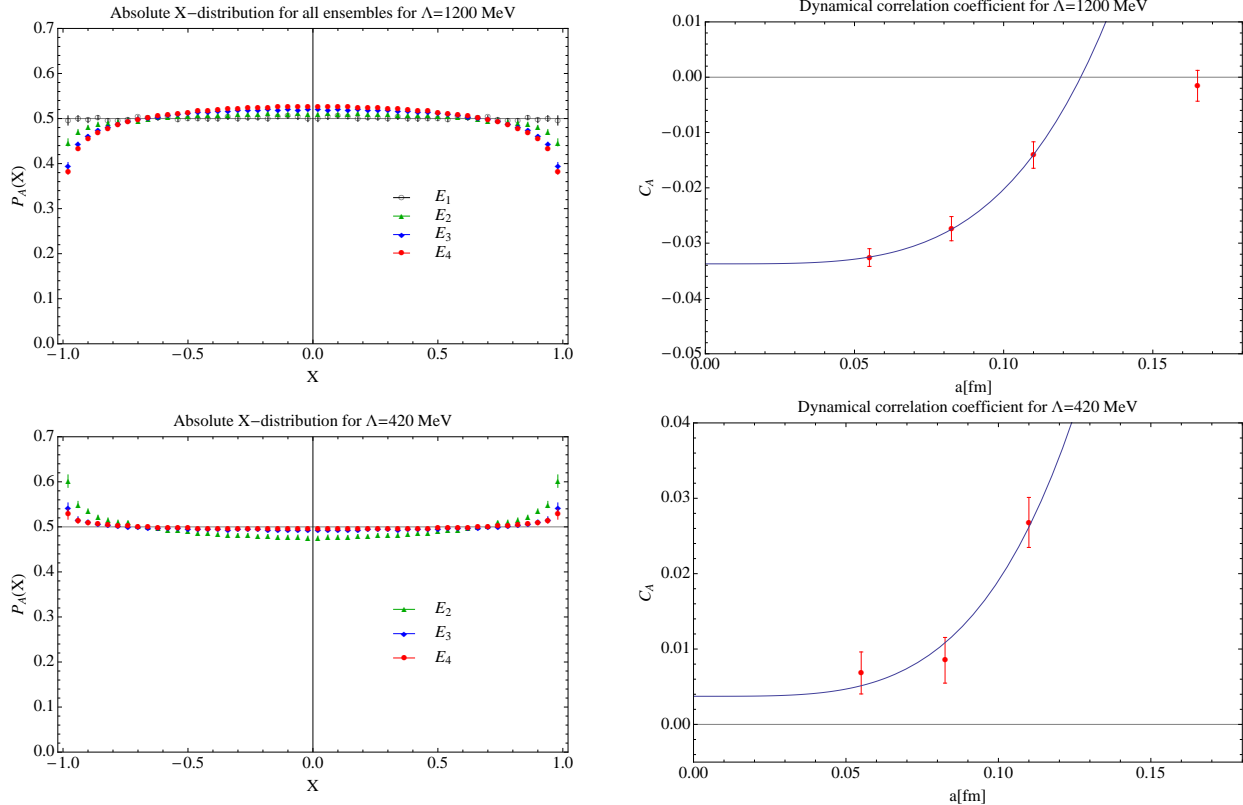


Figure 6: Lattice spacing dependence of absolute X -distributions for overlap Dirac eigenmodes at $\Lambda = 1200$ MeV (top) and $\Lambda = 420$ MeV (bottom). The corresponding correlation coefficients of polarization are shown on the right.

It is naturally expected that this behavior of absolute X -distributions will not depend on the choice of the Dirac operator with exact lattice chiral symmetry. We would also like to emphasize that the weaker statement, namely that the absolute X -distributions are strictly monotonic or constant on each chiral half, might hold not only for low-lying modes but for all Dirac modes.

3.3 Continuum Limit of Distributions at Fixed Λ

Assuming that the dynamics of Dirac eigenmodes at fixed Λ can be assigned a well-defined physical meaning, their dynamical polarization characteristics should have a proper continuum limit. One should point out though that whether this is true or not constitutes the test for the notion of eigenmodes at fixed Λ rather than the test for applicability of absolute X -distributions.

Since our statistics are rather limited, we define the set of modes specifying the dynamics at $\Lambda > 0$ in the following way. For each configuration from given gauge ensemble we take two modes ψ_{λ_i} , $\psi_{\lambda_{i+1}}$ such that $|\lambda_i| \leq \Lambda < |\lambda_{i+1}|$. Here we have ordered the non-zero low-lying modes by magnitude as $\lambda_1, \lambda_1^*, \lambda_2, \lambda_2^*, \dots$. Since in practice one doesn't encounter

any degeneracy of non-zero modes except for conjugate pairs, this definition uniquely picks out the two modes from the spectrum that are “hugging” the value Λ assuming that Λ is sufficiently large ($\Lambda \geq \Lambda_{LOW}^{MAX}$ from Table 1).

In Fig. 6 we show the convergence of absolute X -distributions for eigenmodes at 1200 MeV (top) and 420 MeV (bottom). Note that in case of the latter, the result for ensemble E_1 is not applicable since 420 MeV is less than Λ_{LOW}^{MAX} . This is not a problem because E_1 appears to be too coarse to be used in continuum extrapolations while our aim is to provide the example of the very low Λ . As one can see from plots on the left, the data quite clearly suggests point-wise convergence of absolute X -distributions as the continuum limit is approached. To see this in a more coarse-grained manner, we show in the right column also the lattice spacing dependence of the moment of the distribution (correlation coefficient) in both cases. Their qualitative behavior suggests convergence as well. The lines shown are fits to the form $c_1 + c_2 a^4$ to the points corresponding to E_2 - E_4 . While the power four is suggested by the data at 1200 MeV, the fit should only be viewed to guide the eye. Based on the above, we propose the following for further examination.

Proposition 2 (Continuum Limit): The absolute X -distributions for overlap Dirac modes at scale Λ have a continuum limit in $SU(3)$ pure glue lattice gauge theory.

3.4 Chiral Polarization Transition

The comparison of left and right columns in Fig. 5, as well as the comparison of top and bottom parts in Fig. 6 suggest a high degree of regularity in the dynamical polarization properties of the low-lying modes. In particular, the dynamics of lowest-lying modes always seems to enhance chiral polarization while the dynamics of higher modes tends to suppress it. To check if this is indeed a monotonic feature with respect to scale Λ of the modes, we show in Fig. 7 how the absolute X -distribution for gauge ensemble E_4 changes from low values upwards. As one can see, the transition from convex to concave indeed proceeds in a monotonic manner.

The above behavior is qualitatively similar for all our ensembles and we are thus led to conclude that there exists a sharply defined transition point Λ_T in the spectrum of overlap Dirac eigenmodes, where dynamical polarization properties of these modes qualitatively change. The QCD-inherited dynamics governing the lower part of the spectrum supports chiral polarization while in the upper part it produces chiral anti-polarization. Apart from the mere existence of this dynamical feature, it is quite remarkable that it is not only the CCP that changes sign at Λ_T , but rather the whole polarization dynamics (absolute X -distribution) appears to be indistinguishable (uniform) from statistical independence. This suggests that the existence of this *chiral polarization transition* represents a robust dynamical property of QCD Dirac eigenmodes.

In order to determine Λ_T for our ensembles, we scanned the behavior of CCP with respect to Λ and looked for the behavior in the vicinity of the point where it changes sign. As shown in Fig. 8 for gauge ensemble E_4 , the data suggests linearity in the corresponding region. The transition point was thus determined from the linear fit in this neighborhood. More details about this procedure can be found in Appendix B.

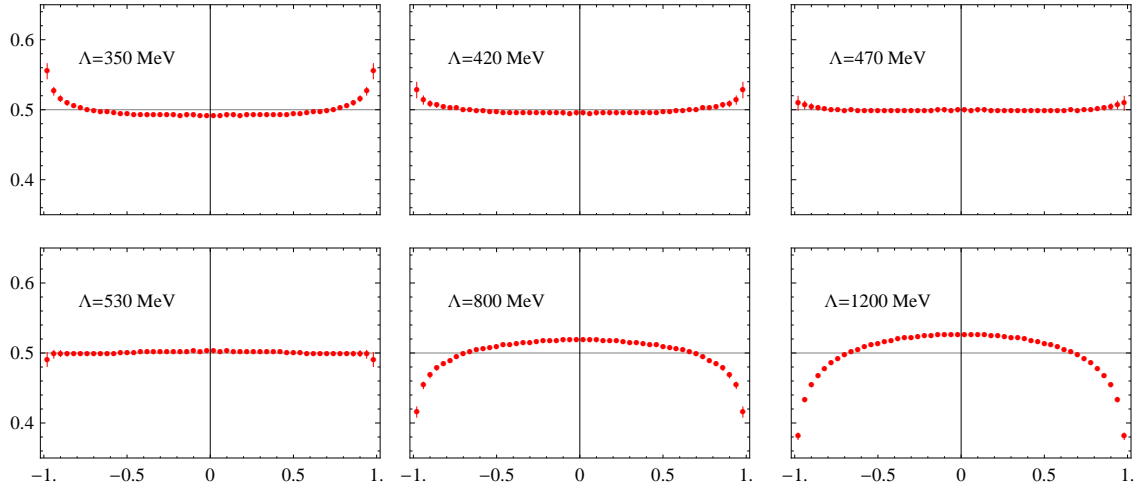


Figure 7: Absolute X -distributions for gauge ensemble E_4 with changing scale Λ of the modes. Note the transition from convex to concave (positive correlation to negative correlation) between 470 MeV and 530 MeV.

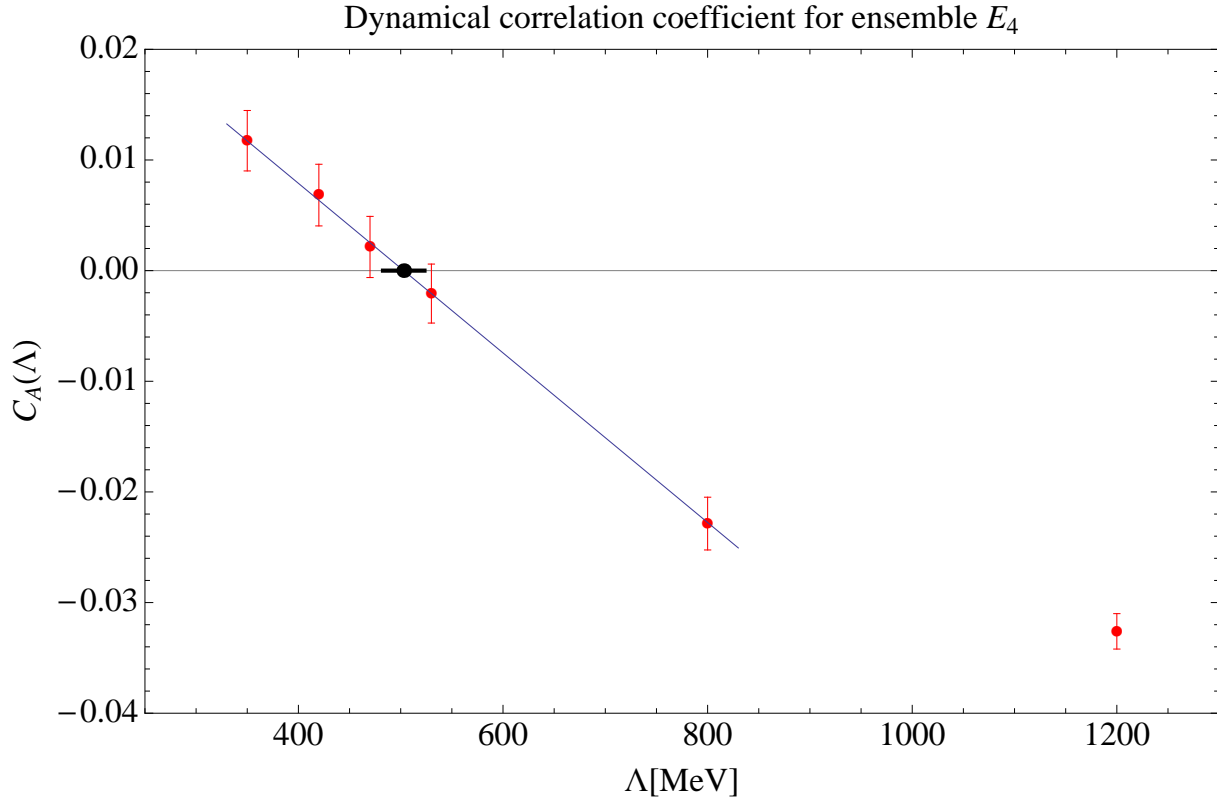


Figure 8: Determination of the chiral polarization transition point Λ_T for ensemble E_4 .

Having performed the determination of Λ_T for ensembles E_1 – E_4 , we show in Fig. 9 the dependence of Λ_T on the lattice spacing. We emphasize that the ensembles in question have fixed physical volume. Our main interest here is to examine whether $\Lambda_T(V, a)$ has a finite continuum limit at fixed V . In other words, whether there is a well-defined finite scale associated polarization dynamics of QCD Dirac eigenmodes in finite volume. As one can see from the figure, our data clearly suggests that this is indeed the case. The fit to $c_1 + c_2 a^4$, with the coarsest ensemble E_1 excluded from the fit, was again used to guide the eye. Based on our results, we propose the following for further investigation.

Proposition 3 (Chiral Polarization Scale): Consider pure glue $SU(3)$ lattice gauge theory in finite physical volume V . There exists a scale $\Lambda_T(V, a)$ in the spectrum of overlap Dirac operator such that its eigenmodes are chirally polarized below $\Lambda_T(V, a)$ and chirally anti-polarized above it. Moreover, the absolute X -distribution changes from convex to concave and is thus uniform at the transition point. The continuum limit $\lim_{a \rightarrow 0} \Lambda_T(V, a)$ exists and is non-zero.

It should be pointed out that the volume of our ensembles is rather small and it is not clear at this point whether the above *chiral polarization scale* remains finite also in the infinite volume limit. We consider this an interesting question that should be studied in the future.

4 Discussion and Conclusions

Polarization tendencies, whether observed empirically in natural phenomena or studied theoretically in various model systems, are frequently of interest in physics. In fact, they are arguably the most basic attributes of dynamical behavior one can attempt to describe. For this reason they are also of interest for the *bottom-up* program of studying QCD vacuum structure [6]. Indeed, the major aspect of this approach is to systematically characterize the properties of the vacuum in a model-independent manner.

Polarization is a highly “coarse-grained” concept and, as such, offers a variety of descriptions that may be consistent with its intuitive meaning. However, such plurality is not necessarily a sign of redundancy. Rather, various descriptions may reflect large freedom in possible aspects of polarization that one could be interested in exploring. Once the intent of the description is meaningfully specified, suitable quantifiers can emerge in a reasonably unique manner. In this work we discussed polarization properties from a different angle. Indeed, rather than looking for description tailored for a specific physical context, our goal was to construct a differential characteristic that is meaningful regardless of what the dynamical variable in question represents. As such, it could then be viewed as an attribute of the dynamics alone, a *dynamical polarization characteristic*.

To achieve the above, we considered a large set of descriptors consistent with the qualitative notion of polarization, namely all possible X -distributions labeled by various polarization functions. If one imagines a rule of assignment associating a suitable description with any given physical context, then the set of X -distributions would be the range of such map: a proper description is always found somewhere within this set. However, given our goals, one should not view different polarization functions as representing all possible physical contexts, but rather as different “reference frames” in which any given dynamics can be looked at in

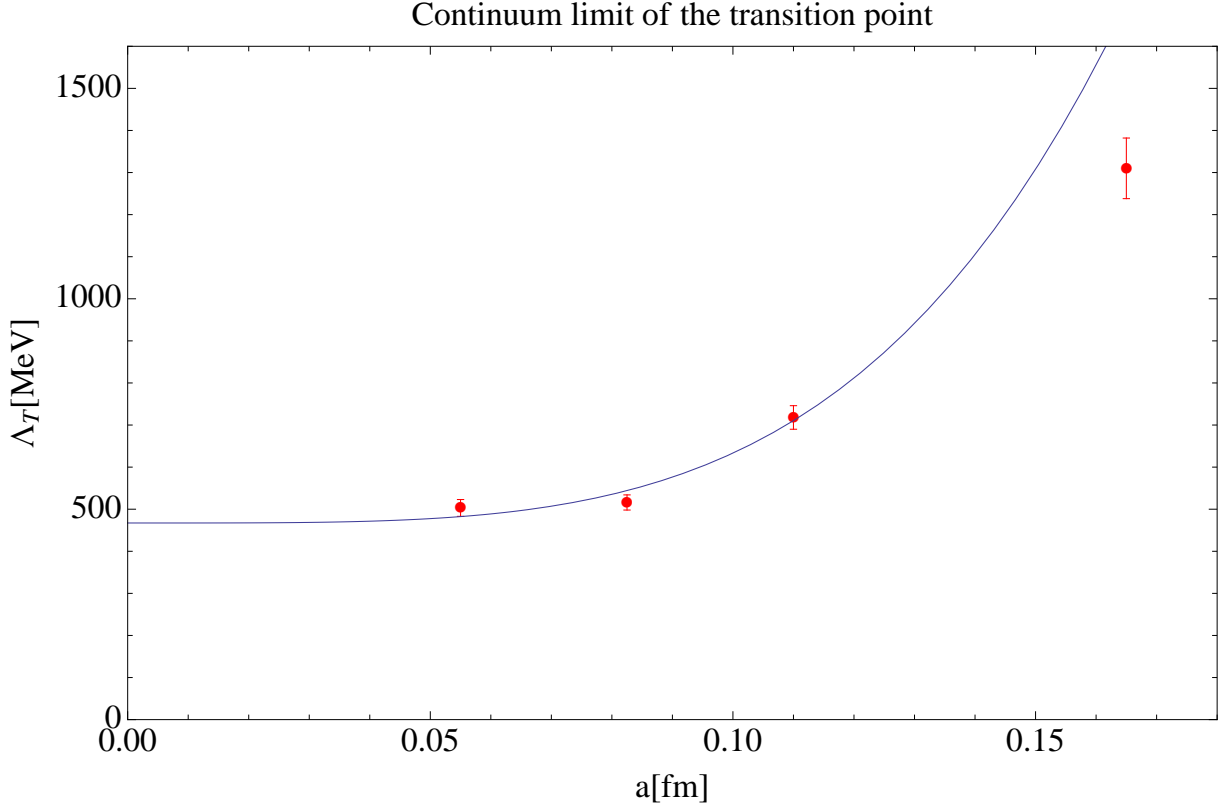


Figure 9: Dependence of chiral polarization point Λ_T on the lattice spacing at fixed volume.

terms of polarization. The X -distribution associated with such a frame is kinematical in the same sense as velocity \vec{v} in given inertial frame is kinematical for mechanical particle: it can be made arbitrary by choosing the reference frame appropriately. The necessary condition for a quantitative measure to be dynamical is its invariance under the change of reference frame, as exemplified by $d\vec{v}/dt$ and its Galilean invariance in case of Newtonian particle. One of our main points in this work is that, for situations involving polarization, the analog of acceleration is the absolute X -distribution with its reparametrization invariance.

Similarly to the case of mechanical particle where one could consider e.g. higher time derivatives, it is possible to construct other X -distributions with reparametrization invariance. Thus, frame independence is not sufficient to fix the dynamical polarization characteristic uniquely. The needed additional requirement we used was that the characteristic be “correlational”. Indeed, as emphasized throughout this article, the absolute X -distribution represents the differential comparison of polarization in given dynamics relative to the case of statistically independent components. If one performs this comparison on average rather than differentially, the correlation coefficient of polarization is obtained. This coefficient can thus be viewed as descending from absolute X -distribution via a coarse-graining procedure. It has a well-defined statistical meaning and provides a suitable measure for ranking of possible dynamics in terms of their dynamical polarization properties.

Somewhat different perspective on our proposal is obtained when one views it as a reduc-

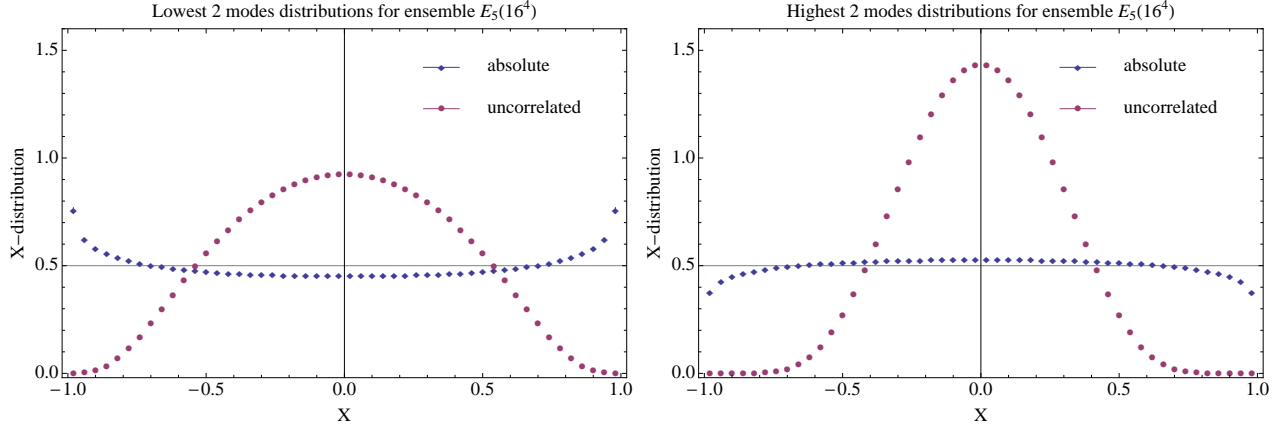


Figure 10: Absolute (dynamical) and uncorrelated (kinematical) X -distributions for gauge ensemble E_5 using the reference polarization coordinate for the latter. Results for lowest two non-zero pairs are shown on the left while the highest two pairs are shown on the right.

tion process wherein the full information on orthogonally decomposed variable $Q \equiv (Q_1, Q_2)$, described by the density function $\mathcal{P}_f(Q)$, is being restricted into the information relevant for describing its polarization properties only. Integrating out unrelated information naturally leads to the notion of polarization dynamics or, equivalently, an X -distribution $P(X)$, but the associated non-uniqueness issues lead to the conclusion that this reduction is in fact insufficient. One should rather consider the reduction to a pair

$$\mathcal{P}_f(Q) \longrightarrow \mathcal{P}_b(q_1, q_2) \longrightarrow P(X), P^u(X) \quad (5)$$

where $P^u(X)$ descends from $\mathcal{P}_f^u(Q)$, namely the distribution of statistically independent components Q_1 and Q_2 . While both members of the above pair vary with the choice of the polarization coordinate, there is an invariant information in the “difference” of the two, and we thus propose that the polarization should rather be characterized by

$$\mathcal{P}_f(Q) \longrightarrow P_A(X), P^u(X) \quad (6)$$

where the first part is invariant (dynamical) and the second part is variant (kinematical).⁶ Note that the kinematical part is still a useful ingredient in the description of polarization. Indeed, if one stores the information on $\mathcal{P}_f(Q)$ in the above form with standard choice of the polarization coordinate, such as $P_A(X)$, $P_r^u(x)$ for reference polarization coordinate, then it is possible to recover all other X -distributions one might need in various physical contexts that this dynamics could be modelling. As an example of such practice, we show in Fig. 10 the polarization characteristics for gauge ensemble E_5 and the group of lowest two (left) and highest two (right) non-zero modes computed. The above conceptual aspects as well as the theoretical structure underlying the method are discussed at length in Appendix A.

⁶Note that, as opposed to pair in (5), the arguments of these two X -distributions have different meanings in this case.

Taking a QCD perspective, it is interesting to apply the above techniques to Dirac eigenmodes and investigate their local chiral structure. This is where the related issues first arose [1]. To this end, we obtained and presented the basic picture of dynamical polarization properties in low-lying overlap Dirac eigenmodes for pure glue QCD. The most intriguing aspect of our findings relates to emergence of new sharply defined feature in the Dirac spectrum, namely that of a *chiral polarization transition*. Indeed, our data indicate that, in finite physical volume, there exists a scale Λ_T in the Dirac spectrum such that QCD dynamics leads to enhancement of local chirality in modes at lower scales, while the same dynamics works to suppress it in modes above the transition. In substantiating this, we focused on continuum limit at fixed physical volume but this basic feature appears to be robust when the volume is increased, as indicated by the results for ensemble E_5 shown in Fig. 10.

Even though it has long been suspected that chirality properties of low-lying Dirac modes are relevant in the mechanism of spontaneous chiral symmetry breaking, it was not known before that QCD dynamics leads to such a clear-cut qualitative distinction in the behavior of low and high parts of the Dirac spectrum. The above result not only confirms the conceptual value of the approach to polarization that we developed here, but also offers what could be a fruitful avenue for “bottom-up” investigation of spontaneous chiral symmetry breaking in QCD. An immediate point of interest in this regard is whether the chiral polarization scale Λ_T remains finite in the infinite volume. Indeed, the existence of such chirality-related scale, generated by QCD dynamics, would open an interesting new class of possibilities for the mechanism of spontaneous chiral symmetry breaking.

Acknowledgments: Ivan Horváth is indebted to Scott Hamann for his support and patience that was important for this work to materialize. Discussions with Robert Mendris are also appreciated. Andrei Alexandru is supported in part by U.S. Department of Energy under grant DE-FG02-95ER-40907. Terrence Draper is supported in part by U.S. Department of Energy under grant DE-FG05-84ER40154. The computational resources for this project were provided in part by the Center for Computational Sciences at the University of Kentucky, and in part by the George Washington University IMPACT initiative.

A General Description of the Method

In this section we describe the absolute X -distribution method in detail. Since the formalism is applicable in a fairly generic setting, we carry this discussion out without reference to a specific physical situation in question. This helps to bring the essential ingredients more to the forefront. Consider a quantity Q taking values in linear space with scalar product. Assume further that there is some physically motivated decomposition of Q into a fixed pair of orthogonal subspaces in place, namely

$$Q = Q_1 + Q_2 \quad Q_1 \cdot Q_2 = 0 \quad (7)$$

where “ \cdot ” denotes the scalar product. What we implicitly have in mind here is that the orthogonal subspaces in question are “equivalent” e.g. of the same dimension, but the resulting methods can be generalized to include non-symmetric cases.

What we mean by specifying the “dynamics” of Q is selecting an arbitrary probability space with allowed values of Q as its sample space. For practical considerations (and manipulations) we will assume however the existence of an underlying probability distribution (function or generalized function) $\mathcal{P}_f(Q)$ from which the probability of measurable events can be obtained via corresponding integrations. It is not important for this discussion whether and how this distribution descended from dynamics of a more complex or fundamental system. For example, in applications related to studying space–time structure of composite fields in QCD (QCD vacuum structure) this probability distribution would have ultimately descended from probability density of gauge configurations given by QCD action.

Since our goal is to describe polarization properties with respect to (7), it is convenient to consider dynamics in terms of the polarization components, i.e. $\mathcal{P}_f(Q_1, Q_2)$. In addition to dynamics, the method we will be describing is built on the notion of a polarization function $\mathcal{X}(Q_1, Q_2)$. The role of \mathcal{X} is to quantify the degree of polarization for any sample (Q_1, Q_2) . One can think of it in terms of a “polarization meter” accepting a sample as an input and providing its polarization value as an output. Different devices of this type are characterized by different polarization functions. In what follows, we will carry out our discussion in the situation where the dynamics are symmetric, namely $\mathcal{P}_f(Q_1, Q_2) = \mathcal{P}_f(Q_2, Q_1)$, and the polarization meters are also symmetric, namely $|\mathcal{X}(Q_1, Q_2)| = |\mathcal{X}(Q_2, Q_1)|$. This is most relevant for our targeted applications. However, we will keep the framework and notation wide enough to incorporate future generalizations in this direction.

Finally, we will be quantifying the tendency for polarization by relative magnitudes of Q_1 and Q_2 . For example, by saying that Q is strongly polarized in the first direction we mean that $|Q_1| \gg |Q_2|$. Consequently, the probability distribution of component magnitudes, namely

$$\mathcal{P}_b(q_1, q_2) \equiv \int dR_1 dR_2 \mathcal{P}_f(R_1, R_2) \delta(q_1 - |R_1|) \delta(q_2 - |R_2|) \quad q_i \equiv |Q_i| \quad (8)$$

will be the object characterizing “dynamics” for our purposes, with the subscript “ b ” in \mathcal{P}_b indicating that this is the representation of dynamics in base sample space variables (q_1, q_2) .

A.1 Polarization Functions

To start with the X -distribution method, one needs to select a suitable function $\mathcal{X}(Q_1, Q_2)$ serving as a measure of polarization on the “sample space”. Such *polarization function* will thus reflect the relative contribution of the two orthogonal subspaces in Q . Due to the linear structure involved, the values of \mathcal{X} assigned to Q and its arbitrary rescaling αQ ($\alpha \neq 0$) should be identical, i.e. we consider Q and αQ to be equally polarized samples. Restricting ourselves to characteristics $\mathcal{X}(q_1, q_2)$ that only depend on magnitudes (q_1, q_2) this translates into the requirement that $\mathcal{X}(q_1, q_2)$ only depends on $t \equiv q_2/q_1$.

Note that, in terms of t , “being smaller” indicates being more polarized with respect to the first direction while “being larger” signals larger polarization with respect to the second direction. Thus, even a simple choice $\mathcal{X}(q_1, q_2) = q_2/q_1$ has some basic features we are seeking. However, we wish to work with characteristics that are symmetric with respect to the two subspaces, and have a standardized compact range. To achieve this, we impose the following set of requirements on acceptable functions \mathcal{X} .

Definition 1 (*Polarization Functions*): Consider real-valued functions $\mathcal{X}(q_1, q_2)$ on $\mathbb{R}_0^+ \times \mathbb{R}_0^+$ where $\mathbb{R}_0^+ \equiv [0, \infty)$. The subset of such functions satisfying the following conditions:

- (a) $\mathcal{X}(q, tq)$ is non-decreasing function of $t \in \mathbb{R}_0^+$ for fixed $q > 0$
- (b) $\mathcal{X}(0, q) = 1$ for $q > 0$
- (c) $\mathcal{X}(q, tq)$ is independent of $q > 0$ for fixed $t \in \mathbb{R}_0^+$
- (d) $\mathcal{X}(q_1, q_2) = -\mathcal{X}(q_2, q_1)$

will be referred to as a set of polarization functions.

Note that, with any polarization function, samples (q_1, q_2) strictly polarized in the first direction ($q_1 > 0, q_2 = 0$), strictly unpolarized ($q_1 = q_2$), and strictly polarized in the second direction ($q_1 = 0, q_2 > 0$) are characterized by functional values $-1, 0$ and $+1$ respectively. \mathcal{X} serves as a comparator in a sense that we say that sample (q_1, q_2) is more polarized than sample (r_1, r_2) if $|\mathcal{X}(q_1, q_2)| > |\mathcal{X}(r_1, r_2)|$. Similarly, given our conventions, we consider sample (q_1, q_2) more polarized in the first direction than sample (r_1, r_2) if $\mathcal{X}(q_1, q_2) < \mathcal{X}(r_1, r_2)$ while we consider it more polarized in the second direction if $\mathcal{X}(q_1, q_2) > \mathcal{X}(r_1, r_2)$. There are obviously infinitely many such comparators (polarization functions).

Every polarization function vanishes at origin $(0, 0)$ and is otherwise specified by the choice of non-decreasing $\mathcal{X}(q_2/q_1) \equiv \mathcal{X}(t)$ such that $\mathcal{X}(t) = -\mathcal{X}(1/t)$ and $\mathcal{X}(0) = -1$. Variable t is in one to one correspondence with the polar angle $\varphi \equiv \tan^{-1}(t)$ in Cartesian plane, and it can thus be useful to parametrize $\mathbb{R}_0^+ \times \mathbb{R}_0^+$ using polar coordinates (ρ, φ) . In this case condition (c) translates into $\mathcal{X}(\rho, \varphi) = \mathcal{X}(\varphi)$. Further simplifications arise by ‘‘symmetrizing’’ the angular variable $\varphi \in [0, \pi/2]$ via rescaled polar angle x of Eq. (2). In this case the remaining conditions on non-decreasing $\mathcal{X}(x)$ translate into $\mathcal{X}(x) = -\mathcal{X}(-x)$ and $\mathcal{X}(1) = 1$. In other words, the set of polarization functions can be faithfully parametrized by odd, non-decreasing functions on $[-1, 1]$ with unit maximal value.

When viewed as functions of x , then simple examples of polarization functions are odd integer powers and their generalizations to positive real powers, namely

$$\mathcal{X}^C(x; \alpha) = \text{sgn}(x) |x|^\alpha \quad \alpha > 0 \quad (9)$$

Note that $\mathcal{X}^C(x; 1) = x$ corresponds to the original chiral orientation parameter of Ref. [1]. When viewed as functions of t , then another simple family of polarization functions is specified by

$$\mathcal{X}^R(t; \alpha) = \frac{t^\alpha - 1}{t^\alpha + 1} \quad \alpha > 0 \quad (10)$$

The special case of $\mathcal{X}^R(t; 2)$ was considered in [3]. Another possibility is to work with

$$\mathcal{X}^G(t; \alpha) = \frac{4}{\pi} \tan^{-1}(t^\alpha) - 1 \quad \alpha > 0 \quad (11)$$

where $\alpha = 1$ is the chiral orientation parameter of Ref. [1] and $\alpha = 2$ was used in [4].

A.1.1 Set \mathbb{X}

Let us denote the set of all odd non-decreasing real-valued functions on $[-1, 1]$ with unit maximal value as \mathbb{X}_0 . Each polarization function is labeled by an element of \mathbb{X}_0 and, in

fact, we will write $\mathcal{X} \in \mathbb{X}_0$ regardless of whether we think of \mathcal{X} in terms of a single variable $\mathcal{X} = \mathcal{X}(x)$, or in terms of two variables $\mathcal{X} = \mathcal{X}(q_1, q_2)$.

Before proceeding, it is useful to make a subtle distinction that will be needed later. Since functions in \mathbb{X}_0 are bounded and non-decreasing, they are continuous except possibly on a countable set of points where they have finite jumps. We will group the functions that only differ by values at points of discontinuity and treat them as a single measure for polarization. To describe the resulting equivalence classes as a new function set, we represent each class by a function that is middle-valued for $|x| < 1$.⁷ We then have the following representation of polarization functions.

Definition 2 (Set \mathbb{X}): Set \mathbb{X} is a subset of real-valued functions $f(x)$ on $[-1, 1]$ satisfying the following conditions:

- (1) $f(x)$ is non-decreasing
- (2) $f(1) = 1$
- (3) $f(x)$ is middle-valued at $|x| < 1$
- (4) $f(-x) = -f(x)$

It should be emphasized that even though $\mathbb{X} \subset \mathbb{X}_0$, it implies a very mild restriction on the set of polarization functions. Indeed, for every element of \mathbb{X}_0 there is an element in \mathbb{X} which differs from it at most on a countable set in domain $[-1, 1]$. The rationale for this restriction is that polarization functions represented by elements of \mathbb{X} are in one to one correspondence with possible polarization dynamics as will be discussed shortly.

A.2 Polarization Coordinates and \mathbf{X} -Distributions

When studying the polarization properties of dynamics $\mathcal{P}_b(q_1, q_2)$ using polarization function $\mathcal{X}(q_1, q_2)$, it is convenient to express probability dependencies directly in terms of \mathcal{X} . In particular, we define the following associated objects

$$\mathcal{P}(X, \rho) = \int_0^\infty dq_1 \int_0^\infty dq_2 \mathcal{P}_b(q_1, q_2) \delta(X - \mathcal{X}(q_1, q_2)) \delta(\rho - \sqrt{q_1^2 + q_2^2}) \quad (12)$$

$$P(X) = \int_0^\infty dq_1 \int_0^\infty dq_2 \mathcal{P}_b(q_1, q_2) \delta(X - \mathcal{X}(q_1, q_2)) \quad (13)$$

$$\Gamma = \int_0^\infty dq_1 \int_0^\infty dq_2 \mathcal{P}_b(q_1, q_2) |\mathcal{X}(q_1, q_2)| \quad (14)$$

where X denotes a generic independent variable parametrizing the range of polarization functions, i.e. $X \in [-1, 1]$, and $\rho \in \mathbb{R}_0^+$ is the magnitude of sample Q . In this way, every polarization function $\mathcal{X}(q_1, q_2) \in \mathbb{X}$ defines a corresponding “sample space coordinate” X which will be referred to as the *polarization coordinate*. We emphasize that the constructs \mathcal{P}, P and Γ depend both on the dynamics \mathcal{P}_b and the polarization function \mathcal{X} . They can thus also be viewed as images of maps $\mathcal{P} = \hat{\mathcal{P}}[\mathcal{P}_b, \mathcal{X}]$, $P = \hat{P}[\mathcal{P}_b, \mathcal{X}]$ and $\Gamma = \hat{\Gamma}[\mathcal{P}_b, \mathcal{X}]$.

⁷Function f will be referred to as middle-valued at x if $f(x) = \lim_{\delta \rightarrow 0^+} (f(x + \delta) + f(x - \delta))/2$. Note that if f is continuous at x then it is also middle-valued. At points of discontinuity with finite jumps, middle-valued function takes a value in the middle of the jump.

By construction, $\mathcal{P}(X, \rho)$ carries the most detailed information about the dynamics $\mathcal{P}_b(q_1, q_2)$ with respect to polarization properties defined by \mathcal{X} , and will be referred to as the *polarization representation*. The other two objects are related to it via the following “descent” relations

$$\mathcal{P}(X, \rho) \longrightarrow \int_0^\infty d\rho \mathcal{P}(X, \rho) \equiv P(X) \longrightarrow \int_{-1}^1 dX |X| P(X) \equiv \Gamma \quad (15)$$

i.e. P is a marginal distribution of \mathcal{P} and Γ is a moment of P (and of \mathcal{P}). In $P(X)$ the information on dynamics unrelated to polarization is integrated out which corresponds to the X -distribution of Ref. [1] generalized to arbitrary \mathcal{X} . X -distributions are central objects of interest in this work. The role of the averaged polarization characteristic $0 \leq \Gamma \leq 1$ will become clear in the upcoming sections.

If $\mathcal{X}(x) \in \mathbb{X}$ is a one to one map of $[-1, 1]$ onto $[-1, 1]$, thus entailing a faithful polarization coordinate on the sample space, then the dynamics specified by $\mathcal{P}(X, \rho)$ is fully equivalent to original $\mathcal{P}_b(q_1, q_2)$. The corresponding subset $\mathbb{X}^f \subset \mathbb{X}$ is comprised of odd, continuous, strictly increasing functions $\mathcal{X}(x)$ on $[-1, 1]$ with unit maximal value. Moreover, utilizing such equivalent parametrizations is particularly efficient if they have a differentiable relationship to base coordinates (q_1, q_2) , since then the standard analytic manipulations in the underlying integrals can be performed. Thus, we also consider the subset \mathbb{X}^{fd} containing those elements of \mathbb{X}^f that are differentiable on their domain, i.e. $\mathbb{X}^{fd} \subset \mathbb{X}^f \subset \mathbb{X}$.

Given the utility of polarization coordinates for our purposes, it is convenient to fix a reference polarization representation of dynamics $\mathcal{P}_b(q_1, q_2)$. Since $x = \mathcal{X}(x) \in \mathbb{X}^{fd}$, the rescaled polar coordinate (2) is particularly suited to play this role.⁸ Changing variables from (q_1, q_2) to (x, ρ) , the associated *reference* polarization representation $\mathcal{P}_r(x, \rho)$ is explicitly specified by

$$1 = \int_0^\infty dq_1 \int_0^\infty dq_2 \mathcal{P}_b(q_1, q_2) = \int_{-1}^1 dx \int_0^\infty d\rho \underbrace{\frac{\pi}{4} \rho \mathcal{P}_b(q_1(x, \rho), q_2(x, \rho))}_{\mathcal{P}_r(x, \rho)} \quad (16)$$

with $q_1(x, \rho) = \rho \cos(\frac{\pi}{4}(x+1))$, $q_2(x, \rho) = \rho \sin(\frac{\pi}{4}(x+1))$. In terms of this representation, equations (12-14) simplify to

$$\mathcal{P}(X, \rho) = \int_{-1}^1 dx \mathcal{P}_r(x, \rho) \delta(X - \mathcal{X}(x)) \quad (17)$$

$$P(X) = \int_{-1}^1 dx P_r(x) \delta(X - \mathcal{X}(x)) \quad (18)$$

$$\Gamma = \int_{-1}^1 dx P_r(x) |\mathcal{X}(x)| \quad (19)$$

where the restricted dynamics $P_r(x) = \int_0^\infty d\rho \mathcal{P}_r(x, \rho)$ focuses on polarization only, and will thus be referred to as the *reference polarization dynamics*. Note that, at the same time, P_r can be thought of as the reference X -distribution.

⁸There are two technical reasons to choose x . First, the change of variables from base pair (q_1, q_2) to polarization pair (x, ρ) doesn't involve x -dependence of the Jacobian. Secondly, the specification of the set of polarization functions in terms of x is simple.

To summarize, we think of all dynamics as being parametrized via distributions $\mathcal{P}_b(q_1, q_2)$ in base coordinates. However, when interested in characterizing polarization properties of \mathcal{P}_b , it is convenient to parametrize the same set of dynamics in the coordinate system that directly reflects the polarization of the sample, which is the role of $\mathcal{P}_r(x, \rho)$. Integrating out the coordinate orthogonal to reference polarization coordinate x , we obtain a restricted dynamics $P_r(x)$ describing polarization only, and we thus view P_r as parametrizing possibilities for polarization dynamics. While it is tempting to take $P_r(x)$ to be a detailed polarization characteristic assigned to dynamics \mathcal{P}_b , the choice of x as a reference polarization coordinate is clearly arbitrary, and we could reparametrize using any polarization function $\mathcal{X}(x) \in \mathbb{X}$. Had we done so, $\mathcal{P}_r(x, \rho)$ would have been replaced by another polarization representation $\mathcal{P}(X, \rho)$, $P_r(x)$ would have been replaced by X -distribution $P(X)$, and the reference value of Γ_r would have changed to Γ . Thus, unlike \mathcal{P}_r , P_r and Γ_r which are assigned to a given dynamics, we view \mathcal{P} , P and Γ as “floating objects” reflecting dependence on \mathbb{X} as well.

A.3 Polarization Dynamics

As emphasized before, the objects of our interest are various X -distributions P that we can assign to given dynamics \mathcal{P}_b , since they carry the information on polarization properties. Given that the polarization dynamics P_r associated with \mathcal{P}_b is itself an X -distribution, it is not surprising that, as seen from Eq. (18), the full information contained in $\mathcal{P}_b(q_1, q_2)$ is not needed to study its X -distributions. Rather, the polarization dynamics $P_r(x)$ represents all we need. We can thus write $P = \hat{P}[P_r, \mathbb{X}]$ instead of $P = \hat{P}[\mathcal{P}_b, \mathbb{X}]$.

Therefore, our analysis in what follows will focus on studying interrelations among the members of the triple (P_r, \mathbb{X}, P) . To do that, it is desirable to be more specific about defining the set of possibilities for polarization dynamics. In particular, we would like to represent them in terms of a function set so that their description is on par with the representation of polarization functions via set \mathbb{X} . In that regard, it is convenient to use the information stored in $P_r(x)$ in the form of the associated cumulative probability function

$$S_r(x) \equiv \int_{-1}^x dy P_r(y) \quad (20)$$

which assigns probability to events $[-1, x]$. We will then consider polarization dynamics represented by $S_r \in \mathbb{P}$ where the function set \mathbb{P} is defined as follows.

Definition 3 (Set \mathbb{P}): Set \mathbb{P} is a subset of real-valued functions $f(x)$ on $[-1, 1]$ satisfying the following conditions

- (1) $f(x)$ is non-decreasing
- (2) $f(1) = 1$
- (3) $f(x)$ is right continuous at all $x < 1$
- (4) $f(x) + f(-x) = 1 + \Delta(x) \quad x > -1, \quad \Delta(x) \equiv f(x) - \lim_{\delta \rightarrow 0} f(x - \delta) \geq 0$

Condition (4) above expresses the symmetry of the underlying dynamics in base variables. The function $\Delta(x)$ detects “atoms” in probability space associated with $f(x)$. In particular, it represents the probability of a point-like event $\{x\}$, which is zero everywhere except possibly on a countable set of points (atoms) where it is positive.

It should be noted that the description in terms of S_r is in fact more general than the description in terms of P_r in the sense that the density representation doesn't exist for all possible cumulative probability functions. Probabilistic spaces with atoms have a discrete part that can be described via distributions (δ -functions), but even in the case when S_r is continuous, it can be non-differentiable on a set of (Lebesgue) measure zero.⁹ In some of such cases a *complete* description of probability space in terms of density simply doesn't exist. Nevertheless, we will interchangeably use both languages since we are not aware of a situation where this distinction would be relevant physically. More importantly, all the constructs considered here can be defined solely in terms of S_r for all elements of \mathbb{P} .¹⁰ Thus the notion of density doesn't even have to be invoked in principle. However, its convenience and physical utility certainly warrant its use.

A.3.1 Polarization Functions – Polarization Dynamics Correspondence

For considerations that will follow, it will be useful to single out polarization dynamics for which $S_r(x)$ is a one to one map of $[-1, 1]$ onto $[0, 1]$. Such subset $\mathbb{P}^f \subset \mathbb{P}$ consists simply of continuous, strictly increasing functions with unit maximal value and satisfying $S_r(-x) + S_r(x) = 1$. Thus, a simple transformation

$$S_r(x) \longrightarrow \mathcal{X}_r(x) \equiv 2 S_r(x) - 1 \quad (21)$$

makes it into odd, continuous, strictly increasing function on $[-1, 1]$ with unit maximal value, namely an element of \mathbb{X}^f . The construction obviously works also in the reverse direction and (21) defines a natural correspondence between polarization dynamics and polarization functions – a bijection between \mathbb{P}^f and \mathbb{X}^f .

Polarization dynamics from \mathbb{P}^f do not contain atoms or events $[x_1, x_2 > x_1]$ with zero assigned probability. The latter can be relaxed while the above correspondence still holds unchanged. Formally, it is then a bijection between larger sets \mathbb{X}^c (\mathbb{P}^c) of continuous polarization functions (dynamics). However, the extension to cases with atoms requires a minor modification. In particular, the problem with (21) then is that the image $\mathcal{X}_r(x)$ is not odd at points of discontinuity due to property (3) of $S_r(x)$, and thus not an element of \mathbb{X} . This is rectified by replacing the map (21) with

$$S_r(x) \longrightarrow \mathcal{X}_r(x) \equiv \begin{cases} 2 S_r(x) - 1 - \Delta(x) & \text{for } |x| < 1 \\ -1 & \text{for } x = -1 \\ +1 & \text{for } x = 1 \end{cases} \quad (22)$$

which only differs from (21) for S_r that are not elements of \mathbb{P}^c . Map (22) in fact defines a bijection between \mathbb{X} and \mathbb{P} , and we can conclude that the freedom in choice of the polarization functions is as large as possibilities for polarization dynamics itself.

A.4 Arbitrariness of Polarization Characteristics

Viewing the constructs \mathcal{P} , P and Γ as tools for characterizing the polarization properties of dynamics \mathcal{P}_b with decreasing level of detail, one has to ask how meaningful these character-

⁹Continuous functions that are not monotonic can be non-differentiable everywhere as exemplified by the famous Weierstrass's function. Monotonicity however greatly reduces options for such exotic behavior.

¹⁰This includes moments, e.g. Γ , as follows from properties of Stieltjes's extension to the Riemann integral.

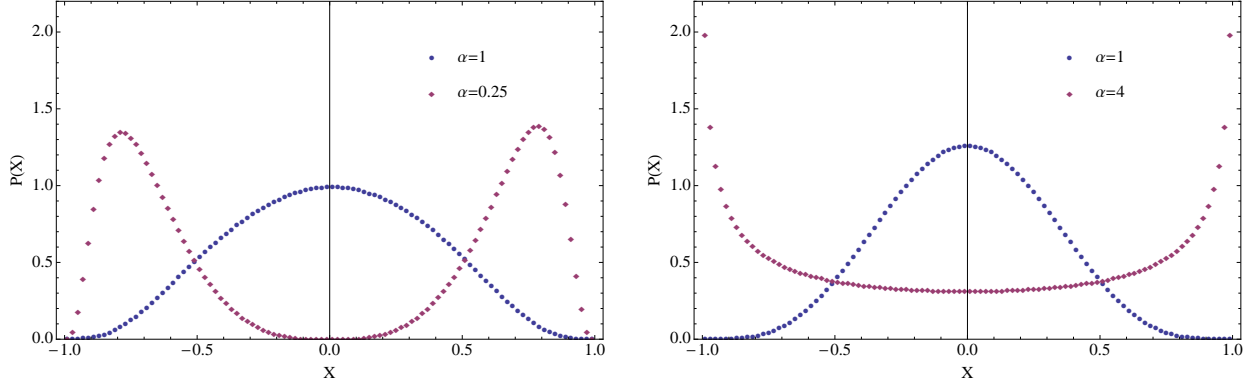


Figure 11: Possible X -distributions associated with fixed dynamics can have qualitatively different behavior. In this example from lattice QCD we selected two polarization functions from family \mathcal{X}^C (left), and two from family \mathcal{X}^R (right).

istics can be since they depend on the choice of the polarization function. In this subsection we will clarify the extent of this arbitrariness in case of X -distributions. Specifically, fixing the polarization dynamics via $P_r(x)$ (or $S_r(x)$), we ask how much can X -distributions $P(X)$ (or $S(X)$) change as we scan the set \mathbb{X} of polarization functions.

To start with a relevant example, we show in Fig. 11 several X -distributions associated with dynamics induced by pure-gluon lattice QCD ensemble E_4 in two pairs of eigenmodes with lowest non-zero eigenvalues (see Table 1 in Sec. 3). The left-right decomposition of Dirac bispinor defines the polarization components, and the details of related calculations are given in Sec. 3. In the left panel we selected two polarization functions from the family \mathcal{X}^C of Eq. (9), with values of α as shown. One can see that the qualitative behavior of the X -distribution differs dramatically for the two choices with $\alpha = 1$ case suggesting a double-peaked (highly polarized) behavior while $\alpha = 1/4$ case exhibiting the opposite (highly unpolarized) tendencies. On the right panel we show a similar example for functions \mathcal{X}^R specified by Eq. (10).

To understand the variability of X -distributions, it is easiest to vary polarization functions within $\mathcal{X}(x) \in \mathbb{X}^{fd}$, i.e. to consider the subset of differentiable faithful polarization coordinates. Then we can make the definition (18) of $P(X)$ more explicit via analytic change of variable to obtain

$$P(X) = \frac{1}{\mathcal{X}'(\mathcal{X}^{-1}(X))} P_r(\mathcal{X}^{-1}(X)) \quad \mathcal{X} \in \mathbb{X}^{fd} \quad (23)$$

where $\mathcal{X}'(x) \equiv d\mathcal{X}(x)/dx$. The form of this result explains why we can obtain wildly varied X -distributions for $P_r(x)$ by changing the polarization function $\mathcal{X}(x)$.

For more general analysis, it is convenient to express the underlying relations in terms of cumulative probability functions. In that case the defining condition for X -distribution $S(X)$ associated with $S_r(x)$ and $\mathcal{X}(x)$ is that it is the probability of the event $\{x | \mathcal{X}(x) \leq X\}$ in the probability space specified by $S_r(x)$. To make this more explicit, notice that if X belongs

to the range $\mathcal{R}[\mathcal{X}] \subset [-1, 1]$ of \mathcal{X} , then $\{x \mid \mathcal{X}(x) \leq X\} = [-1, \bar{\mathcal{X}}(X)]$, a closed interval, while if $X \notin \mathcal{R}[\mathcal{X}]$ then it is an open interval $[-1, \bar{\mathcal{X}}(X))$. Here the generalized inverse $\bar{\mathcal{X}}(X)$ of polarization function $\mathcal{X}(x)$ is defined via the relevant least upper bound, namely

$$\bar{\mathcal{X}}(X) \equiv \sup\{x \mid \mathcal{X}(x) \leq X\} \quad (24)$$

and it coincides with the standard inverse $\mathcal{X}^{-1}(X)$ for $\mathcal{X} \in \mathbb{X}^f$. We then have explicitly

$$S(X) \equiv \begin{cases} S_r(\bar{\mathcal{X}}(X)) & \text{if } X \in \mathcal{R}[\mathcal{X}] \\ S_r(\bar{\mathcal{X}}(X)^-) & \text{if } X \notin \mathcal{R}[\mathcal{X}] \end{cases} \quad (25)$$

where $S_r(x^-)$ is the left limit of S_r at x . The above expression assigns the X -distribution $S(X) \in \mathbb{P}$ to arbitrary $S_r \in \mathbb{P}$ and $\mathcal{X} \in \mathbb{X}$, and is the analog of equation (18). Taking it as a starting point, one can straightforwardly obtain special cases of interest. For example, considering faithful polarization coordinates, i.e. $\mathcal{X} \in \mathbb{X}^f$, we have

$$S(X) = S_r(\mathcal{X}^{-1}(X)) \quad \text{or} \quad S_r(x) = S(\mathcal{X}(x)) \quad \mathcal{X} \in \mathbb{X}^f \quad (26)$$

One use of the above relations is that they show, in an explicit manner, that fixing an invertible polarization function defines a one to one map of \mathbb{P} onto itself, namely a bijection between polarization dynamics and X -distributions. Let us also restrict the polarization dynamics to be from $\mathbb{P}^f \subset \mathbb{P}$ (see section A.3.1) for which the corresponding $S_r(x)$ is a one to one map of $[-1, 1]$ onto $[0, 1]$, and thus invertible. From (26) it then follows that $S(X)$ assigned to $\mathcal{X} \in \mathbb{X}^f$ is an element of \mathbb{P}^f , and thus also invertible. We then have

$$\mathcal{X}(x) = S^{-1}(S_r(x)) \quad \mathcal{X} \in \mathbb{X}^f, \quad S_r \in \mathbb{P}^f \quad (27)$$

The above equation establishes that, given a fixed polarization dynamics S_r from \mathbb{P}^f , we can obtain an arbitrary X -distribution $S(X)$ from \mathbb{P}^f by adjusting the polarization function $\mathcal{X} \in \mathbb{X}^f$ according to (27). In other words, scanning through all polarization functions in \mathbb{X}^f , the constructed X -distributions span the whole \mathbb{P}^f . One can continue further and make this result even more general, but we will not go into additional details. The conclusion is that, for $S_r \in \mathbb{P}^f$, the arbitrariness in its X -distributions is essentially as large as the full variety of polarization dynamics themselves.

The above analysis reveals the simplicity of the structure governing the interrelations in possible triples (S_r, \mathcal{X}, S) when S_r and \mathcal{X} are faithful. In particular, the X -distribution S doesn't have to be thought of as a "dependent variable" determined by S_r and \mathcal{X} , but can be also viewed as an independent object from \mathbb{P}^f . In other words, we have equivalent functional dependencies $S = \hat{S}[S_r, \mathcal{X}]$, $S_r = \hat{S}_r[S, \mathcal{X}]$, and $\mathcal{X} = \hat{\mathcal{X}}[S_r, S]$ whose explicit forms are given above. In what follows, we will implicitly assume the above restriction, i.e. that polarization dynamics are chosen from \mathbb{P}^f , and that polarization functions are chosen from \mathbb{X}^f so that the above structure readily holds. Moreover, when our discussion involves probability densities (P_r or P), the reader can simply assume that we are working in the framework of \mathbb{X}^{fd} and \mathbb{P}^{fd} . However, we emphasize again that everything can be straightforwardly extended to the $\mathbb{P}^f, \mathbb{X}^f$ combination in that case. Most situations of practical interest are covered in this way but when the departure from $\mathbb{P}^f, \mathbb{X}^f$ is necessary, we will explicitly point it out.

A.5 Motivation for Relative Measures

Considerations of the previous section suggest that, in order to meaningfully characterize the dynamics of polarization via X -distributions, one should proceed in one or both of the following ways. (i) Fix the polarization function \mathcal{X} using well-motivated physics considerations, i.e. select polarization function that has direct physical meaning. Whether this can be done depends on the nature of quantity Q in question. (ii) Use only those aspects of X -distributions that do not depend on the choice of the polarization function. We emphasize that (i) and (ii) really represent conceptually different approaches to the issue. The purpose of this paper is to construct universal characteristics of the dynamics in the spirit of the latter. The following considerations turn out to be relevant for achieving that goal.

The feature that puts all polarization functions $\mathcal{X} \in \mathbb{X}^f$ on the same footing is that they are equally good comparators of polarization on the sample space due to strict monotonicity. In other words, if sample (q_1, q_2) was established to be more polarized than (t_1, t_2) using polarization function \mathcal{X}_0 , then this would hold also if any other $\mathcal{X} \in \mathbb{X}^f$ was used to relate them. Thus, any characteristic that may be defined via statistics of such comparisons will be invariant under the choice of the polarization function. To see a simple and useful construct of this type, let us compare the dynamics (distribution) $\mathcal{P}_b^{(1)}$ to dynamics $\mathcal{P}_b^{(2)}$ via the probability Γ_R that a sample drawn from $\mathcal{P}_b^{(1)}$ is more polarized than a sample independently drawn from $\mathcal{P}_b^{(2)}$. While one can approach the determination of Γ_R using different polarization functions, the answer will always be the same. Indeed, this invariance becomes obvious if one pictures evaluation of Γ_R by producing simultaneous draws from $\mathcal{P}_b^{(1)}$ and $\mathcal{P}_b^{(2)}$, and recording the double-sequence of corresponding reference polarization coordinates $\{(x_i^{(1)}, x_i^{(2)}), i = 1, 2, \dots\}$. The relative frequency of encountering $|x_i^{(1)}| > |x_i^{(2)}|$ in this process determines Γ_R , and the result would not change had we tested whether $|\mathcal{X}(x_i^{(1)})| > |\mathcal{X}(x_i^{(2)})|$ instead. Obviously, the information stored in $P_r^{(1)}, P_r^{(2)}$ is sufficient to carry out the above process and in terms of the associated X -distributions we have formally

$$\Gamma_R(P_r^{(1)}, P_r^{(2)}, \mathcal{X}) \equiv \int_{|Y| < |X|} dXdY P(X; P_r^{(1)}, \mathcal{X}) P(Y; P_r^{(2)}, \mathcal{X}) = \Gamma_R(P_r^{(1)}, P_r^{(2)}) \quad (28)$$

where we have made the dependence of various objects on the dynamics and the polarization function explicit everywhere. For obvious reasons, Γ_R will be referred to as the *probability of larger polarization* (PLP) in $\mathcal{P}_b^{(1)}$ relative to $\mathcal{P}_b^{(2)}$.

More detailed invariant objects can be defined using analogous reasoning. One example relevant for our purposes involves the probability $\bar{S}_R(s)$ that a sample drawn from $\mathcal{P}_b^{(1)}$ is more polarized in the first direction than fraction $1 - s$ ($0 \leq s \leq 1$) of the population drawn from $\mathcal{P}_b^{(2)}$. This is invariant with respect to the choice of the polarization function because we can compute $\bar{S}_R(s)$ through the following process. Selecting a reference polarization coordinate as our measure for polarization, we again generate a double-sequence of draws from $\mathcal{P}_b^{(1)}$ and $\mathcal{P}_b^{(2)}$. From the sequence of length N of such draws, namely $\{(x_i^{(1)}, x_i^{(2)}), i = 1, 2, \dots, N\}$, we can obtain an estimate $\bar{S}_R(s, N)$ of $\bar{S}_R(s)$ by first sorting $\{x_i^{(2)}\}$ in ascending order obtaining a sequence $\{x_{j(i)}^{(2)}\}$ of monotonically increasing samples, and setting $x_0 \equiv x_{j(i_0)}^{(2)}$, where i_0 is the smallest index such that $i_0/N > s$. Note that x_0 approximates the separation point where the population from $\mathcal{P}_b^{(2)}$ splits into fraction s of samples most polarized in the first

direction, and the rest. The estimate $\bar{S}_R(s, N)$ is then obtained by counting the relative frequency of occurrences with $x_i^{(1)} < x_0$. It is clear that we could have used arbitrary $\mathcal{X}(x) \in \mathbb{X}^f$ to make all the above comparisons with the same result. Thus, both $\bar{S}_R(s, N)$ and $\bar{S}_R(s) = \lim_{N \rightarrow \infty} \bar{S}_R(s, N)$ are invariant under the choice of the polarization function for all s . To make the contact with X -distributions, we can change the variable and transit from $\bar{S}_R(s)$ to $S_R(X) \equiv \bar{S}_R(1/2 + X/2)$. This resulting object again only depends on the polarization dynamics involved, i.e. we have $S_R(X; P_r^{(1)}, P_r^{(2)})$. We will refer to it as *relative X -distribution* of $\mathcal{P}_b^{(1)}$ relative to $\mathcal{P}_b^{(2)}$. Note that, by construction, if $\mathcal{P}_b^{(1)} = \mathcal{P}_b^{(2)}$, i.e. when comparing given dynamics to itself, we have $\bar{S}(s) = s$ and $S_R(X) = 1/2 + X/2$.

A.6 Relative Measures and their Reparametrization Invariance

Discussion of the previous section fully defines two new objects, namely the probability of larger polarization Γ_R and the relative X -distribution S_R , both assigned to a pair of polarization dynamics from \mathbb{P}^f . However, in order to connect them to previously defined Γ and S , we need to convert the constructive definitions into explicit ones. Let us start by a closer look at equation (28) representing Γ_R which can be written as

$$\begin{aligned} \Gamma_R(P_r^{(1)}, P_r^{(2)}) &= \int_{-1}^1 dx P_r^{(1)}(x) \int_{-|x|}^{|x|} dy P_r^{(2)}(y) = \int_{-1}^1 dx P_r^{(1)}(x) |2S_r^{(2)}(x) - 1| = \\ &= \int_{-1}^1 dx P_r^{(1)}(x) |\mathcal{X}_r^{(2)}(x)| = \Gamma(P_r^{(1)}, \hat{\mathcal{X}}_r^{(2)}) \end{aligned} \quad (29)$$

where $\mathcal{X}_r^{(2)}$ is the polarization function assigned to dynamics $S_r^{(2)}$ (or $P_r^{(2)}$) via natural map (21). Thus the PLP in $P_r^{(1)}$ relative to $P_r^{(2)}$ is the average polarization Γ of $P_r^{(1)}$ in polarization function $\mathcal{X}_r^{(2)}$, as defined by Eq. (19).

To express the relations of the above type, it is convenient to use the ‘‘hat notation’’ for functional prescriptions involving domains of maps (functions) themselves. For example, the functional prescriptions for maps $\hat{S} : \mathbb{P} \times \mathbb{X}^f \mapsto \mathbb{P}$ and $\hat{\mathcal{X}} : \mathbb{P}^f \times \mathbb{P}^f \mapsto \mathbb{X}^f$, introduced via relations (26) and (27) respectively, are given by

$$\hat{S}[S, \mathcal{X}] \equiv S \circ \mathcal{X}^{-1} \quad \text{and} \quad \hat{\mathcal{X}}[S_{(1)}, S_{(2)}] \equiv S_{(2)}^{-1} \circ S_{(1)} \quad (30)$$

where the arguments are to be thought of merely as generic elements of the function sets involved. It is further useful to express the natural map (21) as

$$S \equiv \hat{S}_*[\mathcal{X}] = S_* \circ \mathcal{X} \quad \text{where} \quad S_*(X) \equiv \frac{1 + X}{2} \quad (31)$$

Note that $S_* \in \mathbb{P}^f$ represents polarization dynamics associated with the uniform distribution $P_*(X) = 1/2$, and that $S_r = \hat{S}_*[\mathcal{X}_r]$. According to Eq. (29) we then have, in terms of cumulative probability distributions, that $\Gamma_R = \hat{\Gamma}_R[S_r^{(1)}, S_r^{(2)}]$ with

$$\hat{\Gamma}_R[S_{(1)}, S_{(2)}] \equiv \hat{\Gamma}[S_{(1)}, S_*^{-1} \circ S_{(2)}] \quad (32)$$

Similarly, one can inspect that the construction of the relative X -distribution S_R corresponds to setting $S_R = \hat{S}_R[S_r^{(1)}, S_r^{(2)}]$ with

$$\hat{S}_R[S_{(1)}, S_{(2)}] \equiv \hat{S}[S_{(1)}, S_{\star}^{-1} \circ S_{(2)}] = S_{(1)} \circ S_{(2)}^{-1} \circ S_{\star} \quad (33)$$

Notice that since $\hat{S}[S_r, \mathcal{X}_r] = \hat{S}[S_r, S_{\star}^{-1} \circ S_r] = S_{\star}$, the relative construct $\hat{S}_R[S_{(1)}, S_{(2)}]$ represents a familiar X -distribution for dynamics $S_{(1)}$ with respect to the polarization function for which the X -distribution of $S_{(2)}$ is uniform.

An important feature of the above definitions, discussed in the previous section, is that they are invariant under the choice of the polarization coordinate. In other words, had we chosen a polarization coordinate associated with polarization function $\mathcal{X}(x)$ instead of our reference polarization coordinate x , then the polarization dynamics described by $S_r^{(i)}$ would have been described by its X -distribution $\hat{S}[S_r^{(i)}, \mathcal{X}] = S_r^{(i)} \circ \mathcal{X}^{-1}$ instead. As is obvious from definition (33), the relative X -distribution S_R is invariant under such reparametrization. Consequently, being a moment of associated P_R , PLP is invariant as well.

The basic property of PLP is that

$$\hat{\Gamma}_R[S_{(1)}, S_{(2)}] = 1 - \hat{\Gamma}_R[S_{(2)}, S_{(1)}] \quad (34)$$

as is obvious from its statistical interpretation described in Sec. A.5, and can be easily derived analytically following the definition given above. Similarly, one can immediately see from (33) that the relative X -distribution satisfies

$$\hat{S}_R[S_{(2)}, S_{(1)}] = S_{\star} \circ \left(\hat{S}_R[S_{(1)}, S_{(2)}] \right)^{-1} \circ S_{\star} \quad (35)$$

Thus, up to some necessary modifications by the S_{\star} operation, $\hat{S}_R[S_{(2)}, S_{(1)}]$ and $\hat{S}_R[S_{(1)}, S_{(2)}]$ are inverses of one another, as one can easily understand from the constructive definition of relative X -distribution. We emphasize again that the above relations hold for $S_{(i)} \in \mathbb{P}^f$.

A.6.1 Implementation

Since the definition of absolute X -distribution, to be discussed in the next section, is based on the relative X -distribution, it is worth commenting on the implementation of the latter. The procedure is straightforward if the polarization dynamics $S_{(1)}, S_{(2)}$ (or $P_{(1)}, P_{(2)}$) are explicitly given. Indeed, in that case one simply implements the evaluation of

$$S_R(X) = S_{(1)}\left(S_{(2)}^{-1}(1/2 + X/2)\right) \quad (36)$$

or in terms of probability density

$$P_R(X) = \frac{1}{2} \frac{P_{(1)}\left(S_{(2)}^{-1}(1/2 + X/2)\right)}{P_{(2)}\left(S_{(2)}^{-1}(1/2 + X/2)\right)} \quad (37)$$

However, the explicit forms of relevant distributions are frequently not known in practice. Rather, the dynamics involved are only specified implicitly, e.g. in terms of some reduction

process applied to underlying more complex degrees of freedom. In such situations one typically has an access to the dynamics through a finite probabilistic chain of samples known to be generated from the associated distribution. One option to implement the relative X -distribution in that case is to use the constructive definition given in Sec. A.5. An equivalent approach is to simply follow the original “histogram method” of Ref. [1], and apply it to the probabilistic chain for $P_{(1)}$ and the polarization function

$$\mathcal{X}(x) \equiv 2 \int_{-1}^x dy P_{(2)}(y) - 1 \quad (38)$$

The specifics of the implementation then boil down to the selection of a procedure for approximating $\mathcal{X}(x)$ from a finite probabilistic chain for $P_{(2)}$.

A.7 Absolute X -Distribution

The introduction of relative X -distribution doesn't change the arbitrariness of it as a tool characterizing polarization properties of given dynamics. Indeed, it just moves the arbitrariness in the choice of polarization function into the arbitrariness of the dynamics serving as a comparative standard. However, it does introduce a different angle into the problem that turns out to be useful. Indeed, contrary to the question “Which polarization function should be used?” the question “Which dynamics should we compare to?” does evoke a meaningful answer.

The main idea is as follows. When seeking a characteristic describing a *dynamical tendency for polarization*, what we have in mind is the information on how the projection component behaves in relation to the complementary one, rather than what does it do “in isolation”, or independently of it. In other words, we wish to compare to the dynamics that produces identical answers for any questions involving components “in isolation”, but no effects attributable to the interplay between them. For given dynamics \mathcal{P}_b , such dynamics \mathcal{P}_b^u is uniquely specified, and represents the behavior of statistically independent components with the same distributions of components themselves (marginal distributions). Specifically, denoting the marginal distribution associated with $\mathcal{P}_b(q_1, q_2)$ as $p(q)$, i.e.

$$p(q) \equiv \int_0^\infty dq_2 \mathcal{P}_b(q, q_2) = \int_0^\infty dq_1 \mathcal{P}_b(q_1, q) \quad (39)$$

the corresponding “uncorrelated distribution” \mathcal{P}_b^u is given by

$$\mathcal{P}_b^u(q_1, q_2) \equiv p(q_1) p(q_2) \quad (40)$$

Note that the superscript “ u ” will be used also in other related constructs, i.e. the polarization dynamics associated with \mathcal{P}_b^u will be denoted as P_r^u (or S_r^u). We then define the *absolute X -distribution* associated with dynamics \mathcal{P}_b (in its cumulative form) as

$$S_A = \hat{S}_A[\mathcal{P}_b] \equiv \hat{S}_R[S_r, S_r^u] = S_r \circ (S_r^u)^{-1} \circ S_* \quad (41)$$

namely as X -distribution of S_r relative to S_r^u . There are several remarks regarding this definition that might be useful to emphasize.

(i) The feature that makes the above construction qualitatively different from the old X -distribution approach is that it discards the notion of preferred fixed polarization function. This is obvious from definition (41) corresponding to the choice of the polarization function $\mathcal{X}(x) = 2S_r^u(x) - 1$, which depends on the dynamics \mathcal{P}_b itself. More precisely, the associated polarization function will be the same for members of the equivalence class consisting of all dynamics with fixed marginal distribution in base variables. The members of the same class will be distinguished by their dynamical tendencies for polarization of course, namely by their absolute X -distributions.

(ii) Note that the information in polarization dynamics S_r is not sufficient for constructing the absolute X -distribution for dynamics \mathcal{P}_b . Indeed, the marginal distribution $p(q)$ (and thus S_r^u) cannot be reconstructed from S_r alone. Thus, we cannot scale down from $\hat{S}_A[\mathcal{P}_b]$ to $\hat{S}_A[S_r]$. This is related to point (i) in that for the old “fixed polarization function” approach this is always possible.

(iii) While the notion of absolute polarization function is not viable for characterizing dynamical tendency for polarization, the notion of absolute X -distribution remains. Indeed, the construction (41) is invariant with respect to the choice of the polarization function to implement it. In other words, we could have started with other polarization representation leading to X -distributions S and S^u for \mathcal{P}_b , but we would nevertheless end up with the same absolute X -distribution S_A . At the technical level, this follows from reparametrization invariance of relative X -distributions, and is made obvious by the discussion in subsection A.5.

A.8 Correlation Coefficient of Polarization

The absolute PLP is defined in the same way as the absolute X -distribution, namely

$$\Gamma_A = \hat{\Gamma}_A[\mathcal{P}_b] \equiv \hat{\Gamma}_R[S_r, S_r^u] \quad (42)$$

and can be computed as the moment of the latter (see Eq. (15)). Since Γ_A is an average characteristic based on comparison to statistical independence, it can be thought of as a correlation measure specifically designed for polarization. To be used as such, we define the *correlation coefficient of polarization* (CCP) via

$$C_A \equiv 2\Gamma_A - 1 = S_{\star}^{-1}(\Gamma_A) \quad (43)$$

Note that $C_A \in [-1, 1]$. The positive correlation ($\Gamma_A > 1/2$) signals that dynamics is acting to enhance polarization, while negative correlation ($\Gamma_A < 1/2$) indicates that dynamics works to suppress it. Due to its invariant nature, it quantifies an inherent property of \mathcal{P}_b , namely its overall dynamical tendency for polarization.

A natural question to ask in this regard is why the standard Pearson correlation coefficient is not suitable for this purpose. This is easy to see. Consider the dynamics $\mathcal{P}_b(q_1, q_2)$ with support only on line $q_1 = q_2$. While the Pearson correlation will be perfect ($r = 1$) in this case, it is obvious that there is no dynamical tendency for polarization in such dynamics. In fact, it is just the opposite with dynamics inhibiting any possibility of polarized samples. Indeed, the absolute PLP is obviously zero in this situation for all dynamics with non-singular marginal distributions. These dynamics are thus perfectly antipolarized and characterized by $C_A = -1$ as appropriate.

A.9 Singular Dynamics

At this point we wish to briefly comment on including in the formalism of absolute X -distributions the cases involving dynamics \mathcal{P}_b for which the associated polarization dynamics S_r is not an element of \mathbb{P}^f . Let us recall that there were no restrictions on the notion of standard X -distribution $S(X)$ which can be uniquely assigned to arbitrary $S_r \in \mathbb{P}$ and $\mathcal{X} \in \mathbb{X}$. However, it was natural to focus on the case of bijective maps (elements of \mathbb{P}^f , \mathbb{X}^f), especially as we transitioned to the notion of relative X -distributions. This is reflected in our formulas for $\hat{S}_R[S_{(1)}, S_{(2)}]$, such as (33) and (36), by the presence of $S_{(2)}^{-1}$. In fact, everything discussed in the context of relative X -distributions applies to arbitrary $S_{(1)} \in \mathbb{P}$ and $S_{(2)} \in \mathbb{P}^f$. While this covers most cases of practical interest, it does not afford the construction of absolute X -distributions for \mathcal{P}_b with $S_r \notin \mathbb{P}^f$ since in that case S_r^u is typically not an element of \mathbb{P}^f either.

The main point about the extension from $S_{(2)} \in \mathbb{P}^f$ to $S_{(2)} \in \mathbb{P}$ in the context of relative X -distributions is that it may not simultaneously retain the features coexisting in the former case. In particular, with faithful polarization comparators $S_{(2)} \in \mathbb{P}^f$ we have the interpretation of $\hat{S}_R[S_{(1)}, S_{(2)}]$ both in terms of standard X -distribution with particular polarization function, and in terms of statistical comparisons between the two dynamics, as described in constructive definition of Sec. A.5. In fact, one can easily see that this dual view of the concept extends to the case when $S_{(2)} \in \mathbb{P}^c$. Indeed, the object $S_{\star}^{-1} \circ S_{(2)}$ needed in the definition $\hat{S}_R[S_{(1)}, S_{(2)}] \equiv \hat{S}[S_{(1)}, S_{\star}^{-1} \circ S_{(2)}]$ is a valid polarization function in this case, as discussed in Sec. A.3.1. At the same time, this definition is equivalent to the comparative one in unchanged form.

However, the situation is different when $S_{(2)}$ is discontinuous and thus represents dynamics with probabilistic atoms. The extensions in that case are non-unique in both of the two approaches that become non-equivalent in general. If one follows the rationale of polarization functions, then it is natural to simply extend the S_{\star}^{-1} operation using Eq. (22) and thus define \hat{S}_R via canonical polarization dynamics – polarization function bijection of Sec. A.3.1. When utilizing this definition, then absolute X -distribution assigned to dynamics that one generally thinks of as maximally polarized, i.e. those with $P_{r,p}(x) \equiv \frac{1}{2}\delta(x+1) + \frac{1}{2}\delta(x-1)$, is $P_A^p(X) = P_{r,p}(X)$ and the correlation coefficient is $C_A = 1$. However, if one prefers to focus on the concept of statistical comparisons, then one is led to an alternative path which we now briefly describe.

The root cause of ambiguity in the comparative definitions of Sec. A.5 is that for distributions with atoms, comparisons using “>” and “≥” can become non-equivalent, and one has to fix the treatment of the “=” case. To see the associated issues, let us again consider the polarization dynamics $P_{r,p}$, but assume in addition that the underlying dynamics \mathcal{P}_b has a marginal distribution $p(q) = \frac{1}{2}\delta(q) + \frac{1}{2}\delta(q-1)$. This implies that its uncorrelated polarization dynamics is $P_{r,p}^u(x) \equiv \frac{1}{4}\delta(x+1) + \frac{1}{2}\delta(x) + \frac{1}{4}\delta(x-1)$. Adopting the comparative scheme with sharp inequalities (as we did in Sec. A.5), one immediately obtains that $\hat{\Gamma}_R[P_{r,p}, P_{r,p}^u] = 1/2$ and $\hat{\Gamma}_R[P_{r,p}^u, P_{r,p}] = 0$. On the other hand, admitting the equality always as a positive outcome, we obtain $\hat{\Gamma}_R[P_{r,p}, P_{r,p}^u] = 1$ and $\hat{\Gamma}_R[P_{r,p}^u, P_{r,p}] = 1/2$ instead. Note that in both cases the equation (34) reflecting conservation of probability is not satisfied. In the former case, some probability is “lost” by ignoring the equal outcomes, while in the latter case it is “created” via double counting. The natural approach is to insist that Eq. (34)

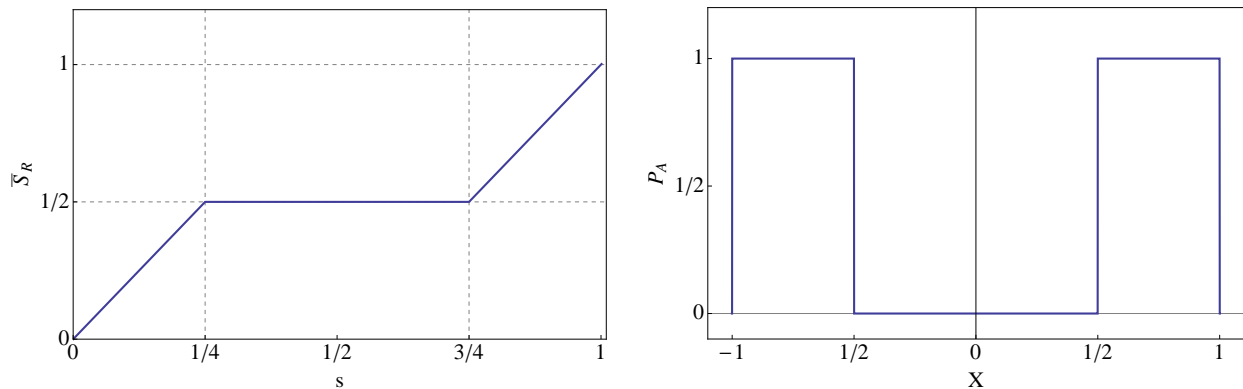


Figure 12: Construction of absolute X -distribution for singular dynamics characterized by $P_{r,p}(x)$ (see text) in the context of statistical comparisons. The intermediate step, $\bar{S}_R(s)$, is shown on the left while $P_A(X)$ is on the right.

be satisfied and that the two dynamics being compared are treated on equal footing. This forces us to assign half of the equal outcomes in favor of first dynamics and the other half to the second dynamics. That way we obtain $\hat{\Gamma}_R[P_{r,p}, P_{r,p}^u] = 3/4$ and $\hat{\Gamma}_R[P_{r,p}^u, P_{r,p}] = 1/4$, implying that $C_A = 1/2$ in this case. We emphasize that while we are focusing on a specific example, the above rule uniquely fixes the assignment of PLP and the correlation coefficient for all possible dynamics.

The above approach can be consistently extended to the level of X -distributions as well. As one can easily check, the construction of Sec. A.5 for relative X -distributions only becomes ambiguous when both dynamics have an atom at the same point x_0 . The proper prescription is that the segment of cumulative probability function associated with such points be linear. Illustrating this again on the case of $P_{r,p}$ and $P_{r,p}^u$, we show in Fig. 12 the construction of \bar{S}_R for $P_{r,p}$ relative to $P_{r,p}^u$, and the associated absolute X -distribution P_A . Note that $\int dX P_A(X) |X| = 3/4 \equiv \Gamma_A$ consistently with the above prescription for PLP.

A.10 More on the Invariance of Absolute Measures

Apart from reparametrization invariance, absolute measures possess additional symmetry that we would like to mention. To do that, it is instructive to think of reparametrization invariance in the following way. Imagine that the generator based on the dynamics $\mathcal{P}_b(q_1, q_2)$ produces the sequence of samples $\{(q_1, q_2)_i\}$, distributed accordingly. The operator of the device broadcasts the sequence to various distant receivers, each of which has a polarization meter at his disposal. When fed a sample $(q_1, q_2)_i$, the polarization meter outputs its degree of polarization X_i , thus allowing each receiver to analyze the polarization properties of \mathcal{P}_b . While the operation of each existing polarization meter is based on a valid polarization function $\mathcal{X} \in \mathbb{X}^f$, there is no standard choice adopted by the manufacturers. Thus, each receiver obtains a different sequence $\{X_i\}$ to work on in general. This would seem to preclude the possibility of producing equivalent polarization characteristics across the spectrum of receivers.

However, every receiver is required to follow special instructions, identical for all, on how to use his polarization meter to determine the *dynamical* polarization properties of the transmitted dynamics. According to this recipe, in addition to running $\{(q_1, q_2)_i\}$ through the polarization meter and producing $\{X_i\}$, he is also required to form an independent sequence¹¹ $\{(q_1, q_2)_i^u\}$, in which the received components are assigned to one another randomly rather than as dictated by the dynamics. The receiver is then to run this randomized sequence through his polarization meter to obtain the associated $\{X_i^u\}$. Finally, he is instructed to perform the statistics of comparisons between X_i and X_i^u to yield the desired dynamical measure of polarization (absolute X -distribution or correlation coefficient). Reparametrization invariance expresses the fact that, assuming they follow the above recipe, all receivers will end up with exactly the same dynamical polarization characteristic.

Thus, by virtue of providing the above instructions, the sender doesn't have to worry about the fact that receivers use various kinds of polarization meters. The additional symmetry of absolute measures pertains to the fact that, to some extent, the same is also true in reverse. In particular, by virtue of the same prescription, the receivers are protected from the fact that the sender could have used various kinds of generators. Indeed, recall that the purpose of the formalism that we developed was to extract from the full dynamics of quantity Q the information on polarization. In doing that, we postulated that the information on dynamics of magnitudes q_1, q_2 of the projections, i.e. $\mathcal{P}_b(q_1, q_2)$, is sufficient for this since the relevant measures are based on the ratios of these magnitudes. However, we could have used the distribution of (q_1^α, q_2^α) ($\alpha > 0$) associated with the same dynamics of Q for this purpose. Thus, different senders communicating information on the same dynamics could have used different kinds of generators and sending the sequence of samples $\{(q_1^\alpha, q_2^\alpha)_i\}$, instead of $\{(q_1, q_2)_i\}$. As one can easily see though, the above recipe for constructing absolute measures guarantees that the result is insensitive to this freedom because the statistics of required comparisons will not change. Formally, these measures are invariant under

$$\mathcal{P}_b(q_1, q_2) \longrightarrow \mathcal{P}_b^{(\alpha)} \equiv \frac{1}{\alpha^2} q_1^{\frac{1}{\alpha}-1} q_2^{\frac{1}{\alpha}-1} \mathcal{P}_b(q_1^{\frac{1}{\alpha}}, q_2^{\frac{1}{\alpha}}) \quad (44)$$

It is due to simultaneous validity of both types of above invariances that we view the constructs discussed here as universal polarization characteristics truly characterizing the dynamics itself, rather than representing our choices for description of polarization.

B Elements of Implementation

In this Appendix we will discuss certain numerical aspects of the results presented in Sec. 3. While the implementation described below was applied specifically to the case of overlap Dirac eigenmodes, one can of course use these strategies in more general settings. We will pay most attention to the computation of absolute X -distributions, but will also discuss the calculation of correlation coefficient C_A and the procedure for the determination of chiral polarization scale Λ_T .

Before we start, it is useful to recall that the input for our calculations is certain dynamics $\mathcal{P}_b(q_1, q_2)$, but we only have a restricted statistical knowledge of it from relevant numerical

¹¹What we mean by “independent” in this case is independent with respect to the ordering of the elements.

simulation. In other words, what we have is a finite population of pairs $\{(q_1^{(i)}, q_2^{(i)}) \mid i = 1, \dots, N\}$, whose statistics is governed by $\mathcal{P}_b(q_1, q_2)$. By virtue of this finite population, the latter can be thought of as being “approximated” by a discrete distribution

$$\begin{aligned} \mathcal{P}_b(q_1, q_2) &\longrightarrow \tilde{\mathcal{P}}_b(q_1, q_2) \equiv \frac{1}{N} \sum_{i=1}^N \delta(q_1 - q_1^{(i)}) \delta(q_2 - q_2^{(i)}), \\ \mathcal{P}_b^u(q_1, q_2) &\longrightarrow \tilde{\mathcal{P}}_b^u(q_1, q_2) \equiv \frac{1}{N} \sum_{i=1}^N \delta(q_1 - q_1^{(i)}) \frac{1}{N} \sum_{j=1}^N \delta(q_2 - q_2^{(j)}) \end{aligned} \quad (45)$$

where the second equation relates to the “uncorrelated” counterpart $\mathcal{P}_b^u(q_1, q_2)$ of $\mathcal{P}_b(q_1, q_2)$. In case of Dirac eigenmodes the population comes from local values in the selected group of modes, such as those at scale Λ in given gauge ensemble, with pairs representing the magnitudes of right and left chiral components.

Our implementation followed the primer calculation described in Sec. 2. Technical details not specified there have to do with the finiteness of the population representing $\mathcal{P}_b(q_1, q_2)$ and the fact that, while one wishes to have its size N as large as possible in order to represent the dynamics adequately, the computational complexity involved in handling the complete information as expressed in Eq. (45) grows as N^2 in case of uncorrelated distribution. Since N can be quite large even with relatively modest size of gauge ensembles, i.e. we have $N \approx 6 \times 10^7$ for ensemble E_4 with only two eigenmodes per configuration contributing, it is computationally advantageous to do some coarse-graining as explained below.

Absolute X -distribution. Given our statistics, we have decided to evaluate $P_A(X)$ at $N_b = 50$ equidistant values based on the information stored in the associated $N_b = 50$ bins of probability. This allows us to plot the distribution with enough resolution to capture relevant details while it also allows for enough statistics in each bin so that the statistical errors are reasonably small. In order to reduce the computational effort, we organized the calculation as follows:

1. Compute the reference polarization coordinates x_1, \dots, x_{N_b-1} representing the boundaries of each bin. To avoid the numerical evaluation of inverse tangent and using the fact that our construction doesn’t depend on the parametrization of the polar angle, we actually work directly with slopes t_1, \dots, t_{N_b-1} ($t \equiv q_2/q_1$). These slopes separate the sample space quadrant into segments containing equal number of samples drawn from the uncorrelated distribution \mathcal{P}_b^u . In Fig. 1 we indicated with solid gray lines these boundaries when the quadrant is partitioned into 10 such bins.
2. Count how many samples $(q_1^{(i)}, q_2^{(i)})$ drawn from the correlated distribution \mathcal{P}_b fall into each bin by comparing their slope with the boundaries determined in the previous step.

Since we only need to inspect each sample once to determine which bin it belongs to, the second step has a complexity $O(N)$, which is negligible compared to the first step which is $O(N^2)$ in the naive implementation. One possibility to deal with the first step is to use a randomly drawn sub-population from the corresponding N^2 samples to approximate the uncorrelated distribution. The problem with this approach is that it interferes with the

error analysis. However, one can organize the calculation carefully and compute the first step using a method that has a complexity only $O(N \log N)$.

The key to this is the ability to compute $S_r^u(t)$ efficiently. Indeed, the problem of finding the boundary is equivalent to solving the equation $S_r^u(t_i) = i/N_b$, and one can solve this equation using a bisection method which can determine t_i to one part in a million with only 20 evaluations of $S_r^u(t)$. To compute $S_r^u(t)$ we sort $\{q_2^{(j)}\}$ in ascending order, a task of complexity $O(N \log N)$. For every $q_1^{(i)}$ we then compute the fraction f_i of elements from $\{q_2^{(j)}\}$ smaller than $t q_1^{(i)}$. Since $\{q_2^{(j)}\}$ is sorted, one can use a binary search which has a $O(\log N)$ complexity. Computing the fraction f_i for all N values of $q_1^{(i)}$ to get the answer $S_r^u(x) = \frac{1}{N} \sum_i f_i$, the total complexity for this task is $O(N \log N)$ as advertised.

While the above strategy makes the calculation of X -distributions manageable, it can still take a considerable amount of time. To speed it up, we sort the values $q_1^{(i)}$ and separate them into bins with equal number of samples. Each bin is then replaced by a single representative value equal to the average of the samples it contains. For the smallest ensemble E_1 where one can comfortably carry out the calculation without binning, we compared the results of the binned version using 1000 elements per bin with the exact calculation. We found that the differences are much smaller than the error bars. For larger ensembles, the approximation is expected to be even better since the number of samples is increased. The binned version was thus used in our evaluations.

The result of the above calculation determines the fraction of samples drawn from \mathcal{P}_b belonging to each of the N_b bins. This information allows us to plot the distribution (histogram) of dS_r/dS_r^u as a function of S_r^u , which can then easily be scaled into the absolute X -distribution $P_A(X)$. To estimate the errors for each value of argument X (or bin), we used single elimination jackknife method with new samples generated by removing one configuration from the gauge ensemble.

The Correlation Coefficient. The evaluation of correlation coefficient C_A is equivalent to the calculation of Γ_A , namely the probability of larger polarization. While Γ_A can be evaluated independently of the absolute X -distribution, we follow its definition as a moment of $P_A(X)$ since this streamlines the error analysis. Every jackknife sample $(P_A)^j$ in the process of calculating the absolute X -distribution produces the jackknife sample Γ_A^j . In particular, if $(P_A)_i^j$ is the value of the estimate for bin i , then we have explicitly

$$\Gamma_A^j = \sum_{i=1}^{N_b} \frac{|X_i + X_{i-1}|}{2} (P_A)_i^j \quad (46)$$

where X_i are the boundaries of the bins that divide the domain $[-1, 1]$ into N_b equal size bins, and thus $X_0 = -1$ and $X_{N_b} = 1$. The jackknife analysis of the above estimates then determines the mean value of the correlation coefficient and its error.

Chiral Polarization Scale. One of the main results in this work is that the correlation coefficient C_A changes sign at a specific scale Λ_T of the eigenmodes. If we denote by $C_A(\Lambda)$, the correlation coefficient evaluated using a pair of eigenmodes $\lambda_{1,2}$ “bracketing” the scale Λ , i.e. $\lambda_1 \leq \Lambda < \lambda_2$, then the chiral polarization transition point is defined via $C_A(\Lambda_T) = 0$. To determine this scale, we first crudely map out the behavior of $C_A(\Lambda)$ by evaluating the correlation coefficient on a grid with steps of about 200 MeV. Note that, using the spectral

information from Table 1, we choose the overall position of these grid points such that all gauge configurations in the ensemble contribute modes for the calculation. Determining the transition region this way, we then evaluate $C_A(\Lambda)$ at few more points in the estimated vicinity of the transition point. Using this information, several values Λ_i closest to the transition are finally selected. The correlation coefficient is then evaluated for each of the jackknife samples and the estimate of the correlation matrix for $C_A(\Lambda_i)$, using a jackknife method, is formed. The final result for Λ_T and its error are evaluated using a linear regression based on this correlation matrix.

Calculation of Eigenmodes. We determine the eigenvalues of the zero-mass overlap operator using our own implementation of the implicitly restarted Arnoldi algorithm with deflation [12]. To speedup the calculation and to reduce the amount of memory required, we compute the eigenvalues of $D^\dagger D = D^\dagger + D$ which is Hermitian and commutes with γ_5 . This allows us to project on a chiral subspace and compute only one member of the chiral pair. The eigenvectors and eigenvalues of the overlap operator are then straightforwardly constructed using the basic properties of the overlap Dirac matrix.

References

- [1] I. Horváth, N. Isgur, J. McCune, H.B. Thacker, Phys. Rev. **D65**, 014502 (2002).
- [2] T. DeGrand, A. Hasenfratz, Phys. Rev. **D65**, 014503 (2002); I. Hip et al., Phys. Rev. **D65**, 014506 (2002); R. Edwards, U. Heller, Phys. Rev. **D65**, 014505 (2002); C. Gattringer et al., Nucl. Phys. **B618** (2001) 205; Nucl. Phys. **B617** (2001) 101; I. Horváth *et al.*, Phys. Rev. **D66**, 034501 (2002).
- [3] T. Blum *et al.*, Phys. Rev. **D65**, 014504 (2002).
- [4] C. Gattringer, *Phys. Rev. Lett.* **88**, 221601 (2002).
- [5] T. Draper *et al.*, Nucl. Phys. **B** (Proc. Suppl.) 140, 623 (2005), [arXiv:hep-lat/0408006](https://arxiv.org/abs/hep-lat/0408006).
- [6] I. Horváth, [arXiv:hep-lat/0605008](https://arxiv.org/abs/hep-lat/0605008).
- [7] I. Horváth, Nucl. Phys. **B710** (2005) 464; Erratum-ibid. **B714** (2005) 175.
- [8] T. Banks and A. Casher, Nucl. Phys. **B169**, 125 (1980).
- [9] Y. Iwasaki, Nucl. Phys. **B258** (1985) 141.
- [10] M. Okamoto *et al.* Phys. Rev. **D60**, 094510 (1999).
- [11] H. Neuberger, Phys. Lett. **B417** (1998) 141; Phys. Lett. **B427** (1998) 353.
- [12] D.C. Sorensen, SIAM J. Matrix Anal. Appl **13** (1992) 357.
R.B. Lehoucq, D.C. Sorensen, SIAM J. Matrix Anal. Appl **17** (1996) 789.